Accepted Manuscript

An integrated study of geochemistry and mineralogy of the Upper Tukau Formation, Borneo Island (East Malaysia): Sediment Provenance, Depositional Setting and Tectonic Implications

Nagarajan Ramasamy, Priyadarsi D. Roy, Franz.L. Kessler, John Jong, Vivian Dayong, M.P. Jonathan

PII: S1367-9120(17)30157-8
DOI: http://dx.doi.org/10.1016/j.jseaes.2017.04.002
Reference: JAES 3038

To appear in: *Journal of Asian Earth Sciences*

Received Date: 25 August 2016
Revised Date: 31 March 2017
Accepted Date: 4 April 2017

Please cite this article as: Ramasamy, N., Roy, P.D., Kessler, Franz.L., Jong, J., Dayong, V., Jonathan, M.P., An integrated study of geochemistry and mineralogy of the Upper Tukau Formation, Borneo Island (East Malaysia): Sediment Provenance, Depositional Setting and Tectonic Implications, *Journal of Asian Earth Sciences* (2017), doi: http://dx.doi.org/10.1016/j.jseaes.2017.04.002

An integrated study of geochemistry and mineralogy of the Upper Tukau Formation, Borneo Island (East Malaysia): Sediment Provenance, Depositional Setting and Tectonic Implications

Nagarajan Ramasamy[a*], Priyadarsi D. Roy[b], Franz. L. Kessler[c], John Jong[d], Vivian Dayong[a], M.P. Jonathan[e]

[a]Department of Applied Geology, Curtin University Malaysia Miri, 98009, Sarawak, Malaysia

[b]Instituto de Geología, Universidad Nacional Autónoma de México, Ciudad Universitaria, CP 04510, Ciudad de México, Mexico.

[c]Goldbach Geoconsultants O & G, Glattbach, Aschaffenburg, Germany.

[d]JX Nippon Oil and Gas Exploration (Deepwater Sabah) Limited, Level 15, Menara Prestige, No. 1, Jalan Pinang, 50450 Kuala Lumpur.

[e]Centro Interdisciplinario de Investigaciones y Estudios sobre Medio Ambiente y Desarrollo, Instituto Politécnico Nacional, Calle 30 de Junio de 1520, Barrio la Laguna Ticomán, Del.Gustavo A. Madero, CP 07340, Ciudad de México, Mexico. Email:

*Corresponding Author: Email: nagarajan@curtin.edu.my; nagageochem@yahoo.com

Mobile: +60 16 525 1245

Abstract

An integrated study using bulk chemical composition, mineralogy and mineral chemistry of sedimentary rocks from the Tukau Formation of Borneo Island (Sarawak, Malaysia) is presented in order to understand the depositional and tectonic settings during the Neogene. Sedimentary rocks are chemically classified as shale, wacke, arkose, litharenite and quartz arenite and consist of quartz, illite, feldspar, rutile and anatase, zircon, tourmaline, chromite and monazite. All of them are highly matured and were derived from a moderate to intensively weathered source. Bulk and mineral chemistries suggest that these rocks were recycled from sedimentary to metasedimentary source regions with some input from granitoids and mafic-ultramafic rocks. The chondrite normalized REE signature indicates the presence of felsic rocks in the source region. Zircon geochronology shows that the samples were of Cretaceous and Triassic age. Comparable ages of zircon from the Tukau Formation sedimentary rocks, granitoids of the Schwaner Mountains (southern Borneo) and Tin Belt of the Malaysia Peninsular suggest that the principal provenance for the Rajang Group were further uplifted and eroded during the Neogene. Additionally, presence of chromian spinels and their chemistry indicate a minor influence of mafic and ultramafic rocks present in the Rajang Group. From a tectonic standpoint, the Tukau Formation sedimentary rocks were deposited in a passive margin with passive collisional and rift settings. Our key geochemical observation on tectonic setting is comparable to the regional geological setting of northwestern Borneo as described in the literature.

Keywords: Geochemistry; Mineralogy; Mineral chemistry; Zircon geochronology; Provenance; Borneo.

1. Introduction

Chemistry of fine-grained clastic sediments provides useful information about provenance, depositional environments (climate and tectonic setting), and post depositional processes (McLennan et al., 1993; Rahman and Suzuki, 2007; Ohta, 2008; Lee, 2009; Nagarajan et al., 2014; Armstrong-Altrin et al., 2015; Sahoo et al., 2015; Zaid, 2015; Pacle et al., 2016; Zhang et al., 2016). However, heavy mineral assemblages are better indicators of provenance compared to the whole rock chemistry as the major and trace element distributions are controlled by multiple and complex mineralogical associations (Mange and Maurer, 1992; Ratcliffe et al., 2007; Sevastjanova et al., 2012). Similarly, chemistry of different heavy mineral grains has also been used to infer provenance of different sedimentary basins (Henry and Guidotti, 1985; Morton, 1991; Asiedu et al., 2000; Weltje and Von Eynatten, 2004; Mange and Morton, 2007; Meinhold et al., 2009; Stern and Wagreich, 2013; Baxter et al., 2016; White et al. 2016). For example, presence of tourmaline indicates granite, granite pegmatite, contact and regionally metamorphosed rocks as the possible provenance. It also relates the provenance to recrystallized schist and gneiss (Mange and Maurer, 1992). Occurrence of chromian spinel suggests mafic and ultramafic provenance (i.e., peridotite, serpentinite and ophiolite) (Irvine, 1965; Dick and Bullen, 1984; Mange and Morton, 2007; Al-Juboury et al., 2009; Meinhold et al., 2009). Thus, an integrated approach involving information of bulk chemistry, mineralogy and mineral chemistry can overcome shortcomings of individual techniques. It can also provide a clear picture of influences of weathering, sorting and maturity on the chemical signatures of any sedimentary basin (Morton et al., 2010).

The Borneo Island is politically divided into Indonesia (Kalimantan), East Malaysia (Sarawak and Sabah) and Brunei. In East Malaysia, thick sedimentary sequences are present in the northern part of the Sarawak province. They were deposited during the Late Paleogene and Neogene and were recycled from accreted deposits belonging to the Rajang Group of central Borneo (Hutchison, 2005; Kessler and Jong 2015a; Jong et al., 2016; Nagarajan et al., 2014, 2015, 2017; Van Hattum et al., 2003, 2013). Sediments of the Rajang Group were exhumed in the Middle Miocene and show phyllite to greenschist facies metamorphism (Hutchison, 1996). These rocks are also referred to as the Rajang fold-thrust belt (Tongkul, 1997). Fragments of ophiolites are likely thrusted within this group (Hutchison, 1996). Apatite and zircon fission track studies by Moss (1998) and Moss et al. (1998) show a relatively subdued burial and exhumation with central ages between 22 and 31 Ma. This interval of rapid cooling (~1.3 km exhumation) occurred in the Late Paleogene and was characterized by a temperature drop of over 40°C in an interval of ~2 Ma.

The northern part of the Rajang Group was uplifted during the Paleogene and became a source for the Neogene sedimentary basins (Morley and Back, 2008). The Schwaner Mountains from western parts of the Sarawak and Kalimantan provinces were the principal provenances and minor additions were derived from ophiolite debris. Heavy mineral suites of these sedimentary rocks were derived from the basement rocks such as granite (Van Hattum et al., 2003). There was a significant change in the sedimentation pattern during the Early Neogene. A large amount of sediments were eroded from the uplifted hinterlands and deposited into the deep foreland basins to the north and east. Major deltas were developed and rapidly prograded from the hinterland (Hall and Nichols, 2002). These sedimentary rocks were recycled from ~10 km thick

nearby elevated basement rocks (Hamilton, 1979; Hall and Nichols, 2002; Morley and Back, 2008). However, Kessler and Jong (2015a) report that the basement rocks were uplifted and eroded to the order of ~6-7 km. Mineralogy and geochemistry of these Neogene sedimentary rocks are poorly studied (Tanean et al., 1996; Van Hattum et al., 2006, 2013; Nagarajan et al., 2014, 2015, 2017). Based on major and trace element compositions, Nagarajan et al. (2014) studied geochemical characters of the Lower Tukau Formation and reported that the sedimentary rocks were of recycled nature with minor ultramafic input. However, it is noted that the mineralogy and the source were not clearly defined for the Neogene sedimentary rocks. Thus, the present study is an integration of new data based on mineralogy and mineral chemistry, and bulk rock geochemistry to better understand provenance, depositional environments and tectonic settings of the Tukau Formation. Apart from helping to establish the potential provenance of the sedimentary rocks, their mineralogical composition would also allow for a better textural and compositional study, where the Tukau Formation represents a key hydrocarbon-bearing reservoir of the producing fields in the study area. The outcomes of the geochemical investigation are helpful in sand-to-sand correlation of the reservoir rocks, especially in ones that are heavily faulted and compartmentalised. Sedimentary rocks of the Tukau Formation are well-exposed and consist of alternations of mudstone and siltstones with occasional quartz pebbles. Their investigations can provide better indications for the provenance compared to separate studies focussing solely on sandstone dominated Lambir Formation, or mudstone dominated formations such as the Sibuti Formation (e.g., Potter et al., 2005). Thus, the main objectives of the present study are: 1) evaluation of mineralogical and geochemical characters of the recycled sedimentary rocks; 2) estimation of the weathering states; and 3) identification of provenance and possible source area of the Neogene sedimentary rocks and the possible tectonic setting.

2. Study Area

The northern Sarawak area hosts Neogene and younger sedimentary rocks, which are exposed towards the north and north-northeast (Fig. 1a, Liechti et al., 1960). The age of the deposits belonging to the Nyalau, Setap, Tangap, Sibuti, Belait, Lambir, Miri and Tukau Formations are in the range from the Oligocene to Pliocene (Fig. 1b). The Tukau Formation is the youngest amongst these deposits (~10-2.58 Ma). The formation overlies a prominent unconformity above the Lambir Formation (Kessler, 2005, 2009a, 2009b) and is exposed near the Bakam and Sungai Rait region located approximately 40 km southwest of Miri (Lat: 4.248586° and Long: 113.959417°; Fig. 1a,b). Lithologically, it has alternate layers of siltstone and mudstone with occasional massive silt/sandstone and mudstone (top of the sequence near Sungai Rait) with thin lenses of coal and quartz pebble beds at the channel base. These pebbles are monomyct and probably derived from hydrothermal quartz veins of the Rajang Group (Kessler and Jong, 2015b, 2016). Pyrite concretions and ambers are common and both of them are present along with iron rich layers. Sedimentary rocks of this formation may have been deposited during the intervals of transgression and regression and tectonic events. Relative absence of planktonic foraminifera suggests that the sedimentary rocks of the Tukau Formation were deposited in shallow marine to deltaic environments (Hutchison, 2005; Kessler, 2009a, 2009b). Similarly, the presence of lignite layers and amber balls indicate that they were deposited on a coastal plain setting (Hutchison, 2005), whilst Kessler (2009a) described the formation as a shoreface deposit.

3. Materials and Methods

3.1 Sampling and sediment bulk chemistry

Different lithological units present in the Upper Tukau Formation were sampled in an exposed profile in northwestern Sarawak (Fig. 1c). A total of 50 samples were selected and processed for measuring major oxides, and trace and rare earth elements (REE). Samples were oven dried at 40^0C, homogenized and subsequently ground to 230 mesh using an agate mortar. Oxides of 10 major elements (Si, Al, Ti, Fe, Ca, Mg, Na, K, Mn and P) were measured in fused discs after the methods of Verma et al. (1996) in Siemens SRS 3000 X-ray fluorescence (XRF) spectrometer with precision of <10% (Roy et al., 2010; Nagarajan et al., 2014). Trace and REE were analysed with ICP and ICPMS. Accuracy and precision for both these analyses were better than 10% except for Sn, Ag and Tl.

3.2 Mineralogy

Identification of bulk minerals, clay minerals and heavy minerals and chemistry of individual minerals were carried out in 20 samples collected from the same outcrops selected for geochemical analyses (11 sandstones, 7 mudstones and 2 mixed/interbedded rocks). All these samples were analysed in Quantitative Evaluation of Minerals by Scanning electron microscopy (QEMSCAN) and 7 samples were analysed in X-ray diffraction (XRD). Significant number of heavy minerals were recovered from 4 samples and subsequently photographed, and individually analysed for their chemical compositions.

For the QEMSCAN analysis, samples were cleaned (oil-free), resin impregnated and prepared as 30 mm polished epoxy resin blocks. Mineral mapping was carried out using a field image technique. The QEMSCAN image analysis software (iDiscover) processed the images and reported the minerals present (see supplementary File 1 for the detailed methodology). XRD was

carried out in two aliquots: whole rock and clay fraction. Aliquot for whole rock analysis was milled and a known quantity of an internal reference (i.e., fluorite) was added to the sample. Addition of an internal standard serves for quality control as well as to quantify amorphous material present in the samples. Samples were micronized and the resulting homogeneous powder was analysed by XRD. Minerals were identified and quantified by the Rietveld refinement method. Clay fraction was concentrated through a combination of ultrasound and centrifugation. The concentrated clay fraction was first analysed by XRD and subsequently re-analysed after glycolation and heat treatments.

3.3 Heavy mineral separation and mineral chemistry

Heavy minerals were concentrated using heavy liquid separation techniques and analysed in scanning electron microscopy (SEM), optical microscopy and QEMSCAN. Grains of chromite, tourmaline and garnet were analysed for chemical compositions. For heavy mineral analysis, the whole rock samples were dried, weighed and crushed to 150 μm size, following the procedures described in the supplementary File 1. Samples were wet screened at 20 μm, dried and weighed. Fraction of >20 μm material was subjected to heavy liquid separation using Tetrabromoethane (TBE) with a specific gravity of 2.96 g/cm³. Sinks were washed with acetone, subsequently dried and weighed. All the material was retained for subsequent analysis. Grains were identified on the basis of backscatter electron brightness and qualitative Energy Dispersive Spectroscopy (EDS) spot chemical analysis. Chromite, tourmaline and garnet were analyzed at a range of accelerating voltages (from 15 kV to 25 kV; typically 25 kV) and beam currents during imaging in order to maximise image quality and optimise EDS spot analysis. Other dense minerals present in the

heavy mineral concentrates (i.e., pyrite and siderite) were excluded from the data set. All data are presented as normalised grain counts, i.e., percentage of a specific mineral.

3.4 Zircon geochronology

Three sandstone samples collected from lower part of the Tukau Formation, near to the boundary of the Lambir Formation, were used for U-Pb dating of zircons at Actlabs, Canada. Ziron grains were concentrated, subsequently embedded in epoxy resin and polished prior to laser ablation analysis using a Resonetics RESOlution M-50 series 193nm excimer laser ablation system equipped with a Laurin Technic Pty S-155 ablation cell. A minimum of 60-70 grains were used for the analysis. The offline data reduction using Vizual Age involved an attempt to find the longest possible integration that yields a concordant point with overlapping $^{206}Pb/^{238}U$, $^{207}Pb/^{235}U$ and $^{207}Pb/^{206}Pb$ ages. A common-Pb correction is also applied whenever necessary and we chose integrations that yield a concordant 204-corrected ellipse (see supplementary File 1). The Plešovice zircon from the Bohemian Massif (Czech Republic) with concordant U–Pb age with a weighted mean $^{206}Pb/^{238}U$ of 337.13 ± 0.37 Ma was used as a standard (Sláma et al., 2008).

4. Results

4.1 Geochemistry

4.1.1 Major element oxide

The modified diagram of Herron (1988) was used to classify the clastic sedimentary rocks. Sedimentary rocks are classified as shale (n=2), wacke (n=24), arkose (n=3), litharenite (n=15) and quartz arenite (n=6) (Fig.2). We have grouped arkose and subarkose together and grouped litharenite and sublitharenite together as the individual fields have limited number of samples.

SiO_2 is the most dominant oxide and it has concentrations of 97.75 wt%; 89.67 wt%; 79.31 wt %; 70.90 wt%; and 64.50 wt% in quartz arenite, litharenite, arkose, wacke and shale, respectively (Table 1). Al_2O_3 is higher in shale (16.29 wt%) and wacke (16.47 wt%) compared to litharenite (6.02 wt.%), arkose (12.69 wt.%) and quartz arenite (1.23 wt.%). Shale has higher K_2O (2.51 wt%) and are depleted in Na_2O (0.10 wt.%). Both CaO and Na_2O are lower (<0.1 wt %) in all the samples. Compared to the upper continental crust (UCC), shale, wacke and arkose have higher TiO_2 and all the rock types have higher SiO_2. Shale is also enriched in Fe_2O_3 compared to UCC and all the other rocks have major oxides lower than UCC (Fig. 3).

4.1.2. Trace element

Transitional trace element (TTE; V, Cr, Co, Ni, Cu and Zn): Shale and wacke have higher concentrations of V (102 and 94 ppm), Co (15.5 and 8.2 ppm) and Ni (35 and 31.7 ppm) compared to litharenite (V: 44.6 ppm; Co: 2.4 ppm; Ni: Below Detection Limit (BDL), arkose (V: 82.3 ppm; Co: 2 ppm and Ni: BDL), and quartz arenite (V: 13.2 ppm; Co and Ni: BDL) (Table 1). Quartz arenite are enriched in Cu (95 ppm) and Zn (160 ppm) and arkose are enriched in Cr (86.7 ppm). Positive correlation between Cr, V and Co with Al_2O_3 and K_2O (Al_2O_3 vs Cr: r =0.8; Al_2O_3 vs: r=0.9; K_2O vs Cr: r=0.7; K_2O vs V: r=0.8 and K_2O vs Co: r=0.6) suggest that transitional trace elements are mainly associated with K-bearing phyllosilicates.

Large ion lithophile element (LILE; Rb, Cs, Ba and Sr): Shale and wacke have higher average concentrations of Rb (118, 114.7 ppm), Cs (8.7 and 9 ppm), Ba (252.5, 240 ppm) and Sr (74.5, 63.5ppm) compared to arkose (Rb: 48.7 ppm; Cs: 7.7 ppm; Ba:213 ppm; Sr: 48.7 ppm)

litharenites (Rb: 48.6 ppm; Cs: 3.6 ppm; Ba: 118.3 ppm; Sr: 41 ppm) and quartz arenites (Rb: 9.3 ppm; Cs: 0.8 ppm; Ba: 35.8 ppm and Sr: 16.2 ppm). Positive correlations of Ba and Rb with K_2O ($r \geq 0.9$), Al_2O_3 ($r \geq 0.90$) and TiO_2 ($r = 0.7$-0.8) suggest the association of large ion lithopile elements in Al, Ti and K bearing minerals (e.g., Feng and Kerrich, 1990; Bauluz et al., 2000; Ali et al., 2014).

High field strength element (HFSE; Zr, Nb, Hf, Ta, Y, Th, U, and W): Arkose (342 ppm), litharenite (250 ppm) and wacke (247 ppm) have higher Zr than shale (205 ppm) and quartz arenite (79 ppm). Distribution of Hf is similar to Zr (arkose: 7.6 ppm; litharenite: 5.8 ppm; wacke: 5.7 ppm; shale: 4.8 ppm; quartz arenite: 2 ppm). Shale has higher Th (12.8 ppm) and U (3.5ppm) followed by wacke (12.6, 3.2ppm), arkose (12.4, 3.4ppm), litharenite (7.6, 2.1ppm) and quartz arenite (2.3, 0.7ppm). Similarly, contents of Y and Nb are higher in shale (28 and 8ppm), wacke (25 and 7.8ppm) and arkose (24 and 5.3ppm) compared to litharenite (14.3 and 4.2 ppm) and quartz arenite (5.3 and 1.8ppm). W is higher in wacke (2.3ppm) and arkose (2 ppm) than litharenite (1.1ppm), shale (1ppm) and quartz arenite (BDL).

Except quartz arenite, tendencies of the UCC normalized trace element concentrations are similar in all the sedimentary rocks (Fig. 3). Quartz arenite and litharenite are enriched with Cu and Zn, and are depleted in all the trace elements. Shale and wacke show an opposite trend. Both are enriched in all the trace elements contents except for Co Ni, Ba and Sr. LILE elements are depleted in all the lithotypes except for Cs. Cs is enriched in shale, wacke and arkoses. HFSE have comparable concentrations in shale, wacke and arkose. All of them are slightly enriched when compared to UCC except for W.

4.1.3. Rare Earth Element (REE)

Wacke (166 ppm), arkose (161ppm) and shale (160 ppm) have comparable ∑REE. Litharenite (93 ppm) and quartz arenite (39 ppm) have ∑REE lower compared to wacke, arkose and shale. Chondrite normalized average REE patterns are characterized by LREE enriched/fractionated (La/Yb_{CN} :7.18-9.27; 2.29-8.83; 7.81-8.20; 5.81-10.81 and 7.21-16.89 for wacke, arkose, shale, litharenite and quartz arenite, respectively), HREE depleted/parallel to subparallel (Gd/Yb_{CN} :1.00-2.15; 0.95-1.35; 1.29-1.65; 0.89-1.35 and 1.01-1.30 for wacke, arkose, shale, litharenite and quartz arenite, respectively) and consistent negative Eu/Eu* anomalies (0.65-0.73; 0.62-0.67; 0.70-0.72; 0.55-0.72 and 0.64-0.75 for wacke, arkose, shale, litharenite and quartz arenite, respectively). REE characteristics of wacke, shale and arkose are comparable to the post Archean Australian Shale (PAAS; Taylor and McLennan, 1985) and UCC (McLennan, 2001). Both litharenite and quartz arenite have less REE compared to PAAS and UCC (Fig. 4). All the REEs show moderate to strong positive correlations ($r \geq 0.6$) with Al_2O_3, K_2O, V, Ga, Rb, Cs, Ba and Th. Both Zr and P_2O_5 show no correlation and negative relationships with REEs.

4.2. Mineralogy

4.2.1. QEMSCAN

Quartz is the major constituent (46-97 wt%). K-feldspar occurs in trace amounts (<1 wt%) and plagioclases are absent. Clay mineral assemblage comprises illite and illite-smectite (1-41 wt%) and minor kaolinite (1.5-9 wt%) (Fig. 5). Chlorite is present in all the samples (0.02 to 9.1wt %) and two samples show high contents (6.3 wt% and 9.1 wt%). Mica (biotite: up to 4%; muscovite: up to 1 wt%) and pyrite (up to 2 wt%) occur sporadically. Heavy minerals include rutile and Ti silicates (anatase), tourmaline, zircon and chromite (see supplementary table 1 for

figure 5 enlarged with only heavy minerals). They have abundances varying between 0.1 and 0.4 wt% with an average of 0.2 wt%. Clay mineral occurs as cements within the sandstone. Kaolinite occurs as lenticular masses scattered throughout the pore network, intermixed with detrital clays in more argillaceous laminae, and also as rounded, grain replacive concentrations. Illite occurs as a grain coating / pore lining cement and may also occur as a detrital phase in association with micas. In addition to clay cements, pore-filling of a number of samples have siderite.

4.2.2. XRD

XRD data are in accord with information obtained in QEMSCAN (Table 2). Quartz is more in whole rock (>2 µm size; 79-97 wt %) and less in clay fraction (<2 µm size 6-56 wt %). On the other hand, illite is present less in whole rock (2-19 wt %) and more in clay fraction (29 – 49 wt %). Illite in whole rock fraction might be detrital illite and mica. Kaolinite is abundant (15-50 wt %) in the clay fraction. Absence of chlorite was possibly because of its abundance below the detection limit (< 3 wt %) of the XRD analysis. Except for in one sample, minor smectite is identified (up to 10 wt %) in the clay fraction.

4.2.3. Heavy Minerals

Out of the 4 analysed samples, significant numbers of heavy minerals were obtained in 3 samples (n=1966; 2449 and 5082 for S02, S07 and S14), in which S02 is arkose and the rest are wacke. A variety of heavy mineral grains with a range of shapes were observed. The common heavy mineral assemblage includes zircon and rutile/anatase and relatively less tourmaline, chromite, ilmenite, monazite, and garnet (Fig.6). In some samples, both xenotime and florencite are

present. Contents of tourmaline, garnet, and florencite broadly follow rutile / anatase. The zircon-rich samples have highest contents of xenotime and monazite.

Textural characteristics (i.e., roundness) suggest different transport distances (recycling) for zircon. Zircon and tourmaline are present as euhedral, highly abraded and rounded crystals (Fig. 7a-i). The detrital zircon grains show sub-rounded to well-rounded morphologies with evidence of mechanical damage by alluvial transport. The euhedral grains of zircon and tourmaline were transported a shorter distance (i.e., nearby sources) (Fig. 7b,c). However, the highly abraded and rounded grains of zircon were transported from sources present at longer distances or from relatively more reworked sources (Fig. 7a, d, g, h). Anhedral (with a pronounced conchoidal fracture for the broken ones) to angular detrital chromian spinels indicate shorter transportation. Some chromite grains have internal dissolution pits (Fig. 7 f, g). Rutile and ilmenite grains also display dissolution features (Fig. 7e-i). Both hematite and goethite are present in the weathered samples.

4.3. Heavy mineral chemistry

Heavy minerals are commonly present in the accessory phase of sediments (<1 wt%). The average chemical composition based on EDS spot quantitative analysis of tourmaline, chromian spinel and garnet grains are presented in Table 3 with their stoichiometric proportions. Composition of tourmalines ranges from dravite (Mg end member) to schorl (Fe end member) (Table 3). Tourmalines are characterized by higher and variable concentrations of Al_2O_3 (33.08-46.85 wt%), SiO_2 (32.19-37.02 wt%) and FeO (6.11-18.53 wt%). MgO is variable and ranges from below detection limit (BDL) of the equipment to 12.45 wt % (avg. 6.62 wt%). TiO_2 content

is also variable as well and ranges from BDL to 4.38 wt% with an average of 1.51 wt%. Na_2O and CaO show distributions of BDL-5.09 wt% (avg. 2.67 wt%) and BDL-1.70 wt% (avg.0.73 wt%), respectively. Tourmaline grains are mostly Fe-rich and some of them are Mg-rich. Chromium spinels are chromites except for one sample and all of them belong to magnesiochromite and hericynite. Cr_2O_3 contents range from 19.27 to 55.88 wt%, and 83% of the grains have Cr_2O_3 > 30 wt% (Table 3). Al_2O_3 contents range from 11.79 to 51.84 wt% with an average of 23.42 wt%. FeO contents range from 11.84 to 35.37 wt% (avg. 25.54 wt%) and MgO ranges between BDL to 16.62 wt% with an average of 7.69 wt%. Cr_2O_3 vs Al_2O_3 and FeO vs. MgO are negatively correlated. TiO_2 content is ranged between 0.44 and 2.50 wt% with an average of 1.19 wt%. Total Fe was measured as FeOt. The ratios of ferrous (Fe^{2+}) and ferric (Fe^{3+}) ions were calculated assuming spinel stoichiometry. The parameters Mg#, Cr# and Fe^{3+}# are defined as $Mg/(Mg+Fe^{2+})$, $Cr/(Cr+Al)$, and $Fe^{3+}/(Cr+Al+Fe^{3+})$, respectively. The Cr# and Mg# ratios vary between 0.20-0.74 (avg.0.55) and 0-0.71 (avg.0.35), respectively. Traces of garnet grains were observed in one sample (i.e., spessartine; MnO=34.2 wt%, Al_2O_3=21.7 wt%, FeO=7.6 wt% and almandine; FeO=29.3 wt%, Al_2O_3=24.9 wt%, MnO=9.8 wt%). Only one sample yielded ilmenite (n=8), and it is enriched in SiO_2 (42.7 wt%) and TiO_2 (33.8 wt%). Ilmenites are also enriched in Al_2O_3 (15.4 wt%) and depleted in FeO (6.1wt%). Na_2O (2.0 wt%) is lower and these ilmenites are leucozene.

4.4. U-Pb dating of zircon grains

The studied zircons were mostly detrital and the U-Pb dating revealed three age clusters for samples from the Tukau-Lambir boundary. Based on $^{206}Pb/^{238}U$ age of <10% discordant data, the youngest group was 117-130 Ma with dominant peaks in 114-119 Ma age range (Lower

Cretaceous). Another age group was of 220-240 Ma with a peak in 225 Ma (Upper Triassic). The older zircons were of 1300-2440 Ma (Meso-Paleo Proterozoic) in age. The conventional U-Pb concordia plots for whole zircon analysis and younger age zircons are presented in Figure 8a and relative frequency plots of youngest zircon ages are presented in Figure 8b. Uranium and Th concentrations in the studied zircons range from 45 - 2300 ppm (avg. 458 ppm) and 25 - 771 ppm (avg. 179 ppm) respectively. U/Th ratio varies between 0.76 and 21.4 with an average of 3.2.

5. Discussion

5.1. Paleoweathering and sediment sorting

Chemical Index of Alteration (CIA; Nesbitt and Young, 1982) and Plagioclase Index of Alteration (PIA; Fedo et al., 1995) are used to evaluate the intensity of weathering. Gradual increase in weathering leads to removal of easily displaced cations (K^+ Na^+ and Ca^{2+}) relative to more stable elements/residual constituents (Al^{3+} and Ti^{4+}) through conversion of feldspar to clay minerals (Nesbitt and Young, 1982). Unweathered and fresh igneous rocks have CIA and PIA values of 45-55 and highly weathered sediments with abundant kaolinite, gibbsite, chlorite and bohemite have CIA and PIA values up to 100. Moderate weathering is reflected by presence of smectite and illite group of clay minerals and CIA and PIA values of 60-80.

Except for one quartz arenite sample, all the sedimentary rocks of the Tukau Formation have uniform and higher values of CIA. CIA varies between 65 and 86 (quartz arenite: 78-86; shale: 84; wacke: 84-86, litharenite: 83-86 and arkose: 82-85) and PIA (93-98) mirrors the CIA values and indicates intensive weathering. Only one quartz arenite sample shows CIA of 65 suggesting

its moderate weathering nature due to high content of iron oxide cement and less clay minerals. Moderate to strong weathering in the source region is also shown by the sample distributions in A-CN-K ternary diagram (Fig. 9). All samples from the Tukau Formation are plotted above the feldspar line and most of them (except quartz arenites) are clustered near the field of illite. Intensive weathering in the source region is also supported by the mineralogical assemblages. Plagioclase is either absent or present in trace amounts. Similarly, clay minerals are more abundant compared to feldspar and ratio of clay/feldspar is higher for all the sedimentary rocks. Mineralogy of the bulk samples shows presence of more illite, less kaolinite and absent to traces of smectite. Some quartz arenites are compositionally more matured and are dominated by quartz.

Illite and chlorite are considered to form by weak hydrolysis and/or strong physical erosion of parent rocks under relatively dry climatic conditions (Galan and Ferrel, 2013; Hu et al., 2014). Similarly, Adatte and Keller (1998) relate the presence of illite in association with quartz and feldspars to detrital origin and deposition in an arid climate. Kaolinite forms under intense weathering and tropical conditions (Biscaye, 1965; Wan and Chen, 1988). Illite present in the Tukau Formation sedimentary rocks shows both moderate and poor crystallinity. Moderately crystalline illites indicate predominantly physical weathering. It was not degraded further and lacked neoformation (Gaucher, 1981). The poorly crystalline illites were formed due to intense hydrolysis in the hinterland source area under warm humid climatic conditions. More kaolinite in two arkose samples (i.e., S01 and S08) indicates intensive hydrolysis under warm and humid climate. During the Oligocene-Miocene, active tectonic setting of the northern Borneo favoured stronger physical erosion of parent rocks (Hutchison, 2005; Rangin et al., 1990). The intense

seasonal precipitation also supported physical erosion and deposition of illite and chloite dominated clay minerals (i.e., Liu et al., 2012). In addition, the moderate chemical weathering of recycled sediments increased the abundance of kaolinite in some samples. In the QEMSCAN analysis, kaolinite occurs as pore-lining to filling and commonly as a grain replacive authigenic phase, whilst illite occurs both as pore-lining cement and also as possible detrital material (i.e., in the more argillaceous laminae). Trace amounts of smectite can be either detrital or *in situ* formation through early diagenesis, alteration of volcanic glasses and hydrothermal activity (e.g., Ehrmann et al., 2005).

The A-CN-K plot indicates that all the sedimentary rocks were derived from felsic dominated cratons. Additionally, the deviation of some samples from the weathering trend towards K_2O in the A-CN-K diagram can be interpreted as provenance mixing with more continental signature (Cox et al., 1995). Higher average values of Rb/Sr (wacke: 1.8; shale: 1.6; litharenite: 1.2; arkose: 2.0; quartz arenite: 0.6) indicate intense weathering and recycling history. Weathering and sediment recycling increase the Rb/Sr values (McLennan et al., 1993). Surface textures of chromian spinels indicate the combined effects of mechanical attrition and chemical etching during the transportation. Subhedral habit with evidence of dissolution and presence of grooves indicate higher degree of chemical weathering. The observed conchoidal fractures in chromian spinels were formed as a result of mechanical weathering. Immature chemical weathering of the ophiolites under highly oxidizing and alternating wet/dry conditions or metamorphosed ophiolites such as serpentinites might be the sources for the chromian spinel present in the Tukau Formation.

The Al_2O_3-TiO_2-Zr ternary plot (Fig. 10) illustrates fractionation of zircon related to sorting (Garcia et al., 1994). The Tukau sedimentary rocks plot towards Zr and are characterized by changes in Al_2O_3/TiO_2 ratio (Fig. 10). Zr is mainly controlled by zircon and it is enriched due to sorting and recycling (Basu et al. 1990; McLennan et al. 1993). Detrital zircon present in the Paleogene sandstones of southern Borneo was derived from the Schwaner Mountains (Williams et al., 1988) and it was recycled further to the north during the Neogene (Van Hattum et al., 2003). SiO_2/Al_2O_3 ratio estimates the sediment maturity as it reflects the quartz abundance at the expense of primary clay minerals (McLennan et al., 1993). Both the quartz arenite and litharenite show higher maturity compared to arkose, wacke and shale. The zircon-tourmaline-rutile (ZTR) index proposed by Hubert (1962) is used to estimate the mineralogical "maturity" of the heavy mineral assemblage. The ZTR index (>95) also indicate that sedimentary rocks of the Tukau Formation are highly matured.

5.2. Provenance

Sedimentary rocks of the Tukau Formation contain abundant rutile/anatase and zircon, plus minor amounts of chromite. Zircon grains display a range of shapes ranging from the pristine euhedral crystals to rounded and heavily abraded grains. Variable shapes suggest that the zircon grains were derived from several sources (of different ages) and/or might have undergone extensive transport and/or reworking. In the Tukau Formation, zircon was sourced from the felsic igneous rocks and rutile was derived from high-grade metamorphic rocks. Minor amounts of chromian spinels were sourced from the ultramafic/mafic rocks such as veins or embedded masses in peridotites and serpentinites. Presence of both euhedral and well-rounded grains of heavy minerals suggests a mixture of metamorphic/metasedimentary and granitic rocks as the

possible sources with minor influence from the ultramafic/mafic rocks. Heavy mineral ratios such as garnet/zircon (GZi: 5.5-24.7) and rutile/zircon (RuZi: 38.6-87.2) also support a metasedimentary source (i.e., and/or metamafic rocks) and/or an acid igneous rock (i.e., allanite bearing granitoid) as the possible sources (e.g., Ratcliffe et al., 2007).

Major elements based discrimination diagrams of Roser and Korsch (1988) also suggest a mixed provenance. Most of the samples fall in quartzose sedimentary provenance field and only two shale samples plot in mafic igneous provenance. This indicates that source rocks were mainly of felsic nature with minor contribution from mafic-ultramafic rocks (Fig. 11). Felsic source and the recycled nature of the sedimentary rocks are reaffirmed by the Hf vs La/Th plot of Floyd and Leveridge (1987). Increasing concentration of Hf indicates recycled/old sedimentary passive margin source or progressive dissection of an arc (Fig. 12). Wackes plot mostly in acidic arc field and are comparable with UCC and PAAS. One quartz arenite sample falls in mixed felsic and mafic sources indicating some contribution from the mafic to ultramafic sources. According to Kessler and Jong (2016), large quartz pebbles of the Tukau Formation were possibly derived from the Belaga Mountains, composed of clastics of the Rajang Group and some hydrothermal quartz veins. The same source possibly provided the large quartz pebbles during the hinterland uplift and exhumation since the Late Miocene (Kessler and Jong, 2015a).

The felsic dominated source rocks from the source region is also confirmed by REE systematics: LREE enriched, HREE depleted, negative Eu/Eu* anomaly and higher values of LREE/HREE (Fig. 4). The obvious negative Eu anomalies reflect sources that had experienced fractionation of feldspar. It suggests a granitoids dominated provenance for the first cycle of sedimentation.

Litharenites and arkoses have Eu/Eu* values similar to PAAS (Eu/Eu*=0.6-0.7) and values of this anomaly are higher (Eu/Eu*=0.6-0.7; 0.7 and 0.6-0.8) for wacke, shale and quartz arenite. The higher values are due to recycling and dissolution of more feldspar in a second cycle of weathering (e.g., Hassan et al., 1999). Mongelli et al. (2006) reported that Eu released during the feldspar dissolution are retained by clay minerals and thus reduce the Eu anomaly. Lower K_2O/Al_2O_3 ratio (<0.2), enrichment of LREE/HREE values (>8) and less soluble elements (i.e., Th and Y), and depletion of highly soluble elements (i.e., U and Sr) suggest recycling (e.g., Cox and Lowe, 1995; Cox et al., 1995).

Contribution of mafic-ultramafic rocks from the source region was evaluated by concentrations of Cr, V, Ni, Sc (Cullers, 2000) and ratios of Y/Ni and Cr/V (Hiscott, 1984). Higher Cr (>150 ppm) and Ni (>100 ppm) are indicators of ultramafic sources (Garver et al., 1996). Cr content of 40-87 ppm and Ni of ≤40 ppm in wacke, shale, litharenite, arkoses, and quartz arenite indicate less or no significant input from ultramafic source rocks. However, one wacke sample with higher Cr (12D; 230 ppm) and presence of chromian spinels suggest a significant input from mafic-ultramafic rocks. Shale and some wacke received minor input from mafic/ultramafic sources and both have MgO > 1% and Cr+Ni ≤ 260ppm.

In addition to mineralogy and bulk rock geochemistry, chemistry of tourmaline and chromian spinels was also used to reconstruct the provenance. As tourmaline is stable in both weathering and diagenetic environments, chemistry of detrital tourmaline based provenance discrimination diagrams (Fe-Mg-Al and Fe-Mg-Ca; Henry and Guidotti, 1985) were used to evaluate similarities and differences between detrital tourmaline populations and the nature of source

areas (Morton and Hallsworth, 2007). The tourmalines fall in fields B and D of the Al-Mg-Fe plot (Fig. 13a) and plot in fields 2 and 4 in the Fe-Mg-Ca plot (Fig. 13b). Both indicate that the tourmalines were predominantly derived from metasedimentary rocks (metapelites, metapsammites, alumunious) with subordinate input from Li poor granitoids, pegmatites and aplites.

The detrital chromian spinels are characterized by Cr# and Mg# >0.5 and <0.5 and <0.5 and >0.5, respectively. It corresponds to both Al rich chromite composition (≤ 0.6) and Cr-rich chromite compositions (≥ 0.6) (Proenza et al., 2008). Spinels with Cr# <0.5 are derived from lherzolitic bodies (such as the abyssal peridotites of slow spreading ridges (Lee, 1999), and also from back arc basins (Cookenboo et al., 1997). In the Al_2O_3 vs. Cr_2O_3 diagram, many samples plot in podiform field (Fig. 14a) and in the transition between stratiform and podiform fields. It suggests that the chromian spinels are mainly derived from the Alpine type ophiolite. In Cr^{3+}, Al^{3+} and Fe^{3+} triangular plot (Fig. 14b), all the samples are in Alpine type peridotite field which indicates the signature of ophiolites crystallized in a forearc setting (Lenaz et al., 2000). The Alpine type peridotites are similar to podiform type and are richer in Al and Cr^{3+} and have lower Fe^{3+} (Lee, 1999). Comparable with the present study, Hutchison (2005) reported that abundance of chromian spinels was lower in peridotite and serpentinized peridotite in northern Borneo. Similarly, the Cr# vs Mg# plot shows that chromian spinels were mainly derived from metamorphosed ophiolites and some of them were sourced from lherzolites (Fig. 14c). In the Al_2O_3 vs TiO_2 diagram of Kamenetsky et al. (2001), chromian spinels of the Tukau Formation fall in island-arc basalts and Mid-Oceanic Ridge Basalts (MORB) type volcanic rocks (Fig. 14d). Serpentinized peridotites of northern Borneo are comparable to the Alpine type peridotites.

Hence, the Alpine type serpentinized peridotites (e.g., Lupar ophiolites within the Rajang accretionary complex) were one of the possible sources for the studied chromian spinels.

Three zircon age clusters of this study are comparable to age clusters reported for the Crocker and Rajang Group of sediments by Van Hattum et al. (2013). Cretaceous and Triassic were the two major age clusters. The first age cluster can be related to the Schwaner pluton, whilst the second cluster can be related to plutons from the Malaysia Peninsular. The older zircons might have sourced from a more distal source (e.g., Indo-Australian plate) and possibly undergone several recycling phases. The Schwaner plutons are widely accepted as source rock for the Borneo Orogenic Belt. Ages of these plutons range from 130±2.8 Ma to 77.4±1.7 Ma (Williams et al., 1988; Van Hattum et al., 2006; Witts et al., 2012; Li et al., 2015). According to White et al. (2016), samples collected within Borneo yielded dominant age populations between 75 and 110 Ma. Comparable ages of both suggests that the Schwaner Mountains were the principal source rocks for the Rajang Group of rocks and were subsequently recycled further north and northwest of Borneo during the Neogene.

In addition to the Schwaner Mountains, granitoids of the Malaysia Peninsular is another possible source area. The Bentong-Roub suture (consisting of serpentinites, deeps sea radiolarian cherts and Middle Devonian to Late Permian sedimentary rocks) divides granitoids of the Malaysia Peninsular into Main Range and Eastern provinces (Ng et al., 2015 and references provided there in). Eastern province granitoids have U-Pb zircon ages of 289-220 Ma with some younger ages (~80 Ma). The Main Range province magmatism was constrained between 219 and 198 Ma (Ng et al., 2015). According to the same authors, a progressive westward younging trend was apparent across the Eastern province and it was less obvious in the Main Range province. The

Main Range granites of the Malaysia Peninsular consist of tin-bearing S-type granites of Triassic age (Bignell and Snelling, 1977; Liew and Page, 1985) and the Eastern provinces are dominated by I-type granite of Permian-Triassic age (Searle et al. 2012 and references provided there in). Similarly, the southwestern Thailand-Myanmar province granites are mixture of tin bearing S-type and I-type plutons of the Cretaceous age. Zircon age of the Tukau Formation is comparable to the Main Range granites rather than the southwestern Thailand-Myanmar province. In different studies, detrital cassiterites (tin bearing mineral) were found in the Crocker range sediments (Van Hattum et al., 2013) as well as the Neogene sediments of northwestern Borneo (Nagarajan et al., 2015). It supports that the tin bearing granitoids were one of the major possible sources for the sediments of Crocker-Rajang accretionary complex. Identification of the Schwaner Mountains and peninsular Main Range as source rocks for the sedimentary rocks of central Borneo and their subsequent recycling for the Neogene deposits of northern Borneo is in agreement with the previous studies by Van Hattum et al. (2003, 2013) and White et al. (2016).

5.3. Tectonic setting

The tectonic history of Borneo is complex and yet to be fully understood. However, several authors (e.g., Hall, 2002, 2009; Hall et al., 2008; Cullen, 2010; Morley et al., 2003; Hutchison, 1996, 2005) have suggested occurrence of major tectonic events affecting the study area. The Sarawak Orogeny caused change in sedimentation as a transition from flysch to molasse occurred in northwestern Borneo during the Late Eocene (Hutchison, 2007). During this event, turbidite flysch of the Rajang Group were folded, thrusted and uplifted (Kessler and Jong, 2015a, 2015b; Jong et al., 2016). During the Early Miocene, the proto-South China Sea rifted; both rifting and subduction were subsequently slowed and the Borneo landmass was uplifted further.

According to Kessler and Jong (2015a), transition from the muddy Middle Miocene shelf (Setap Shale and Sibuti Formation) to an unusual sandy formation during the Middle to Late Miocene can be attributed to tectonic compression. Regional tectonism in addition to climatic influence enhanced the erosion of Rajang/Crocker Formations and deposited sand-rich sedimentary rocks. The northern part of Borneo possibly had a collisional tectonic setting at the time and the passive rifts might have developed along faulted margins in the zones of continental collision (e.g. Ingersoll, 1988). Rifts are common along the collisional boundaries due to irregularities of continental margins and by normal faulting due to nonperpendicular collision (e.g., Condie, 2011).

Many discrimination diagrams have been proposed to discriminate the active and passive margin settings (Bhatia, 1983; Bhatia and Crook, 1986; Roser and Korsch, 1986, 1988). All samples from the Tukau Formation are plotted in passive margin field of the K_2O/Na_2O-SiO_2 (recalculated to 100% volatile free; Roser and Korsch, 1986) discrimination diagram (Fig. 15). However, Totten et al. (2000), Armstrong and Verma (2005), Ryan and Williams (2007), Pe-piper et al. (2008), Von Eynatten et al. (2012), Verma and Armstrong-Altrin (2013, 2016) and Basu et al. (2016) have cautioned as the proposed discrimination plots do not always successfully classify the correct tectonic settings. Recently, Verma and Armstrong-Altrin (2016) proposed a new tectonic discrimination diagrams based on log ratio transformation and linear discrimination analysis of an extensive geochemical database from the Neogene-Quaternary siliciclastic sediments from the active and passive margin tectonic settings. In this study, all the samples fall in the passive margin setting in the major oxides based plot, whereas some of the

samples plot in the active tectonic setting boundary in the major - trace element based discriminant plot (Fig. 16).

6. Conclusion

New data on bulk mineral, heavy mineral, mineral chemistry and bulk rock geochemistry for sedimentary rocks of the Tukau Formation of the Borneo Island in East Malaysia were used for an integrated study to identify provenance, estimate paleo-weathering and infer tectonic setting during the Neogene. More specifically;

i. Sedimentary rocks are dominated by wacke and shale is present in minor abundance. Mineralogical and geochemical indices (ZTR, CIA and PIA) characterize these sedimentary rocks as highly matured and the source area has undergone moderate to intensively weathering.

ii. Zircon chronology of the Tukau Formation has two young age populations: Cretaceous and Triassic. The Schwaner Mountains and Tin Belt of the Malaysia Peninsular have comparable ages. Granitoids present in both of them were the important sources for the Rajang Group, which further recycled during the Neogene and minor contribution came from mafic and ultramafic rocks present in the Rajang Group.

iii. We postulate that the Tukau Formation was deposited in a passive margin with minor deviation towards an active margin boundary. In addition to tectonic settings, climate (chemical weathering) played a major influence on chemistry of these sedimentary rocks.

Acknowledgements

The authors would like to convey their utmost appreciation to JX Nippon Management for the financial assistance for carrying out mineralogical analyses as part of a broader provenance study of the northwest Borneo region. Rufino Lozano-Santacruz of the Institute of Geology (UNAM) carried out XRF analysis. This study was partially supported by Curtin Sarawak Research Performance fund awarded to the first author. We would like to thank our reviewer Dr. Inga Sevastjanoa and the editor for their valuable comments, which have improved the quality of the manuscript significantly. We extend also our upmost appreciate to Mr. Steven Barker for a final linguistic review of the revised manuscript.

References

Adatte, T., Keller, G., 1998. Increased volcanism, sea-level and climatic fluctuations through the K/T boundary: mineralogical and geochemical evidences. In: Abstracts, International seminar on recent advances in the study of Cretaceous sections, ONGC, Regional Geoscience Laboratory, Chennai, pp.2.

Ali, S., Stattegger, K., Garbe-Schönberg, D., Frank, M., Kraft, S., Kuhnt, W., 2014. The provenance of Cretaceous to Quaternary sediments in the Tarfaya basin, SW Morocco: Evidence from trace element geochemistry and radiogenic Nd–Sr isotopes. Journal of African Earth Sciences 90, 64-76. doi:10.1016/j.jafrearsci.2013.11.010.

Al-Juboury, A.I., Ghazal, M.M., McCann, T. 2009. Detrital chromian spinels from Miocene and Holocene sediments of northern Iraq: provenance implications. Journal of Geosciences 54, 289–300. doi:10.3190/jgeosci.041.

Armstrong-Altrin, J.S., Nagarajan, R., Balaram, V., Natalhy-Pineda, O., 2015. Petrography and geochemistry of sands from the Chachalacas and Veracruz beach areas, western Gulf of Mexico, Mexico: Constraints on provenance and tectonic setting. Journal of South American Earth Sciences 64, 199-216. doi: 10.1016/j.jsames.2015.10.012.

Armstrong-Altrin, J.S., Verma, S.P., 2005. Critical evaluation of six tectonic setting discrimination diagrams using geochemical data of Neogene sediments from known tectonic settings. Sedimentary Geology 177, 115–129. doi:10.1016/j.sedgeo.2005.02.004.

Asiedu, D.K., Suzuki, S., Shibata, T., 2000. Provenance of sandstones from the Lower Cretaceous Sasayama Group, Inner Zone of Southwest Japan. Sedimentary Geology 131, 9–24. doi: 10.1016/S0037-0738(99)00122-0.

Basu, A., Bickford, M.E., Deasy, R., 2016. Inferring tectonic provenance of siliciclastic rocks from their chemical compositions: A dissent. Sedimentary Geology 336, 26–35. doi: 10.1016/j.sedgeo.2015.11.013.

Basu, A.R., Sharma, M., DeCelles P.G., 1990. Nd, Sr-isotopic provenance and trace elements geochemistry of Amazonian foreland basin fluvial sands, Bolivia and Peru: Implications for ensialic Andean orogeny. Earth and Planetary Science Letters 100, 1–17. doi: 10.1016/0012-821X(90)90172-T.

Bauluz, B., Mayayo, M.J., Fernandez-Nieto, C., Gonzalez Lopez, J.M., 2000. Geochemistry of Precambrian and Paleozoic siliciclastic rocks from the Iberian Range (NE Spain): implications for source-area weathering, sorting, provenance, and tectonic setting. Chemical Geology 168(1-2), 135–150. doi: 10.1016/S0009-2541(00)00192-3.

Baxter, A.T., Aitchison, J.C., Ali, J.R., Chan, J.S.L., Chan, G.H.N., 2016. Detrital chrome spinel evidence for a Neotethyan intra-oceanic island arc collision with India in the Paleocene. Journal of Asian Earth Sciences 128, 90–104. doi: 10.1016/j.jseaes.2016.06.023.

Bhatia, M.R., 1983. Plate tectonics and geochemical composition of sandstones. Journal of Geology 91, 611–627.

Bhatia, M.R., Crook, K.A.W., 1986. Trace element characteristics of graywackes andtectonic setting discrimination of sedimentary basins. Contributions to Mineralogy and Petrology 92, 181–193. doi:10.1007/BF00375292.

Bignell, J.D., Snelling, N.J., 1977. The geochronology of Malayan granites (Overseas Geology and Mineral Resources). Institute of Geological Sciences (Great Britain), H.M. Stationery Office, 71pp. ISBN: 0118807552, 9780118807555.

Biscaye, P.E., 1965. Mineralogy and sedimentation of the recent deep-sea clay in the Atlantic Ocean and adjacent seas and oceans. Geological Society of America Bulletin 76, 803–832. doi: 10.1130/0016-7606(1965)76[803:MASORD]2.0.CO;2.

Bonavia, F.F., Diella, V., Ferrario, A., 1993. Percambrian podiform chromitites from Kenticha Hill Southern Ethiopia. Economic Geology 88, 198-202. doi:10.2113/gsecongeo.88.1.198.

Condie, K.C., 2011. Earth as an Evolving planetary system (2nd Ed.) Elsevier, Great Britain, 574pp. ISBN: 978-0-12-385227-4.

Cookenboo, H.O., Bustin, R.M., Wilks, K.R., 1997. Detrital chromian spinel compositions used to reconstruct the tectonic setting of provenance: implications for orogeny in the Canadian Cordillera. Journal of Sedimentary Research 67, 116–123. doi: 10.1306/D4268509-2B26-11D7-8648000102C1865D.

Cox, R., Lowe, D.R., 1995. A conceptual review of regional-scale controls on the com-position of clastic sediment and the co-evolution of continental blocks and their sedimentary cover. Journal of Sedimentary Research 65, 1–21.

Cox, R., Lowe, D.R., Cullers, R.L., 1995. The influence of sediment recycling and basement composition on evolution of mudrock chemistry in the southwestern United States. Geochimica et Cosmochimica Acta 59(14), 2919–2940. doi: 10.1016/0016-7037(95)00185-9.

Cullen, A., 2010. Transverse segmentation of the Baram-Balabac basin, NW Borneo: refining the model of Borneo's tectonic evolution. Petroleum Geoscience 16, 3-29. doi: 10.1144/1354-079309-828.

Cullers, R.L., 2000. The geochemistry of shales, siltstones and sandstones of Pennsylvanian-Permian age, Colorado, U.S.A.: implications for provenance and metamorphic studies. Lithos 51, 181-203. doi: 10.1016/S0024-4937(99)00063-8.

Dick, H.J.B., Bullen, T., 1984. Chromian spinel as a petrogenetic indicator in abyssal and alpine-type peridotite and spatially associated lavas. Contributions to Mineralogy and Petrology 86, 54–76. doi:10.1007/BF00373711.

Ehrmann, W., Setti, M., Marinoni, L., 2005. Clay minerals in Cenozoic sediments off Cape Roberts (McMurdo Sound, Antarctica) reveal palaeoclimatic history. Palaeogeography, Palaeoclimatology, Palaeoecology 229, 187–211. doi: 10.1016/j.palaeo.2005.06.022.

Fedo, C.M., Nesbitt, H.W., Young, G.M., 1995. Unraveling the effects of potassium metasomatism in sedimentary rocks and paleosols, with implications for weathering conditions and provenance. Geology 23(10), 921-924. doi: 10.1130/0091-7613(1995)023<0921:UTEOPM>2.3.CO;2.

Feng, R., Kerrich, R., 1990. Geochemistry of fine grained clastic sediments in the Archaean Abitibi greenstone belt, Canada: implication for provenance and tectonic setting. Geochimica et Cosmochimica Acta 54, 1061–1081. doi: 10.1016/0016-7037(90)90439-R.

Floyd, P.A., Leveridge, B.E., 1987. Tectonic environments of the Devonian Gramscatho basin, south Cornwall: framework mode and geochemical evidence from turbidite sandstones. Journal of the Geological Society London 144, 531-542. doi: 10.1144/gsjgs.144.4.0531.

Galán, E., Ferrell, R.E., 2013. Genesis of Clay Minerals, In: Bergaya, F., Lagaly, G. (Eds.), Handbook of Clay Science (2nd Ed.), Part A: Fundamentals. 5, pp. 83-126. (Chapter 3). doi:10.1016/B978-0-08-098258-8.00003-1.

Garcia, D., Fonteilles, M., Moutte, J., 1994. Sedimentary fractionation between Al, Ti, and Zr and genesis of strongly peraluminous granites. Journal of Geology 102, 411–422.

Garver, J.I., Royce, P.R., Smick, T.A., 1996. Chromium and nickel in shale of the Taconic Foreland: a case study for the provenance of fine-grained sediments with an ultramafic source. Journal of Sedimentary Research 66, 100-106. doi: 10.1306/D42682C5-2B26-11D7-8648000102C1865D.

Gaucher, G., 1981. Les facteurs de la pédogenèse. Traité de pédologie agricole, tome II, Éditions G. Lelotte-Dison, Belgique, 730pp.

Hall, R., 2002. Cenozoic geological and plate tectonic evolution of SE Asia and the SW Pacific: computer-based reconstructions, model and animations. Journal of Asian Earth Sciences 20, 353–431. doi: 10.1016/S1367-9120(01)00069-4.

Hall, R., 2009. The Eurasian SE Asian margin as a modern example of an accretionary orogeny. In: Cawood, P.A., Kroner, A. (Eds.), Earth Accretionary Systems in Space and Time, Geological Society of London Special Publication 318, pp. 351–372. doi: 10.1144/SP318.13.

Hall, R., Nichols, G.J., 2002. Cenozoic sedimentation and tectonics in Borneo: climatic influences on orogenesis. In: Jones S.J., Frostick, L. (Eds.), Sediment Flux to Basins: Causes, Controls and Consequences. Geological Society of London Special Publications 191, pp. 5–22. doi: 10.1144/GSL.SP.2002.191.01.02.

Hall, R., Van Hattum, M.W.A., Spakman, W., 2008. Impact of India–Asia collision on SE Asia: the record in Borneo. Tectonophysics 451, 366–389. doi: 10.1016/j.tecto.2007.11.058.

Hamilton, W., 1979. Tectonics of the Indonesian region. U.S. Geological Survey, Professional Papers, 1078.

Hassan, S., Ishiga, H., Roser, B.P., Dozen, K., Naka, T., 1999. Geochemistry of Permian Triassic shales in the Salt range, Pakistan: implications for provenance and tectonism at the Gondwana margin. Chemical Geology 168, 293–314. doi: 10.1016/S0009-2541(99)00057-1.

Henry, D.J., Guidotti, C.V., 1985. Tourmaline as a petrogenetic indicator mineral: An example from the staurolite grade metapelites of northwest Maine. American Mineralogist 70, 1–15.

Herron, M.M., 1988. Geochemical classification of terrigenous sands and shales from core or log data. Journal of Sedimentary Petrology 58(5), 820–829. doi: 10.1306/212F8E77-2B24-11D7-8648000102C1865D.

Hiscott, R.N., 1984. Ophiolitic source rocks for Taconic-age flysch: trace element evidence. Geological Society of America Bulletin 95, 1261–1267.

Hu, B., Li, J., Cui, R., Wei, H., Zhao, J., Li, G., Fang, X., Ding, X., Zou, L., Bai, F., 2014. Clay mineralogy of the riverine sediments of Hainan Island, South China Sea: Implications for weathering and provenance. Journal of Asian Earth Sciences 96, 84–92. doi: 10.1016/j.jseaes.2014.08.036.

Hubert, J.F., 1962. A zircon-tourmaline-rutile maturity index and independence of composition of heavy mineral assemblages with gross composition and texture of sandstone. Journal of Sedimentary Petrology 32, 440-450.

Hutchison, C.S., 1996. The ‘Rajang accretionary prism’ and ‘Lupar Line’ problem of Borneo. In: Hall, R., Blundell, D.J. (Eds.), Tectonic Evolution of Southeast Asia. Geological Society of London Special Publication 106, pp. 247–261. doi: 10.1144/GSL.SP.1996.106.01.16.

Hutchison, C.S., 2005. Geology of North-West Borneo; Sarawak, Brunei and Sabah. Elsevier, Amsterdam, 421pp.

Hutchison, C.S., 2007.Geological Evolution of South-East Asia. 2nd ed., Geological Society of Malaysia, Kuala Lumpur, 433pp. ISBN 978-983-99102-5-4

Ingersoll, R.V., 1988. Tectonics of sedimentary basins. Geological Society of America Bulletin 100, 1704–1719. doi: 10.1130/0016-7606(1988)1.

Irvine, T.N., 1965. Chromian spinel as a petrogenetic indicator, part I: theory. Canadian Journal of Earth Sciences 2(6), 648–672. doi: 10.1139/e65-046.

Jong, J., Kessler, K.L., Noon, S., Tan, T.Q., 2016. Structural development, depositional Model and petroleum system of Paleogene carbonate of the Engkabang-Karap Anticline, onshore Sarawak. Berita Sedimentologi 34, 5-46.

Kamenetsky, V.S., Crawford, A.J., Meffre, S., 2001. Factors controlling chemistry of magmatic spinel: an empirical study of associated olivine, Cr-spinel and melt inclusions from primitive rocks. Journal of Petrology 42, 655–671.

Kessler, F.L., 2005. Comments on the evolution of Bukit Lambir area; PGCE bulletin, Kuala Lumpur.

Kessler, F.L., 2009a. Shape parameters of clay and quartz clasts in the Neogene Tukau and Lambir Formations. Warta Geologi 35(4), 127-130.

Kessler, F.L., 2009b. Observations on sediments and deformation characteristics of the Sarawak Foreland, Borneo Island. Warta Geologi 35(1), 1-10

Kessler, F.L., Jong, J., 2015a. Tertiary uplift and the Miocene evolution of the NW Borneo shelf margin. Berita Sedimentologi, 33, 21-46.

Kessler, F.L., Jong, J., 2015b. Incision of rivers in Pleistocene gravel and conglomeratic terraces: Further circumstantial evidence for the uplift of Borneo during the Neogene and Quaternary. Bulletin of the Geological Society of Malaysia 61, 49–57.

Kessler, F.L., Jong, J., 2016. Shape parameters of clay and quartz clasts in the Neogene Tukau and Lambir Formations, NW Sarawak. Warta Geologi 42(3-4), 63-68.

Lee Y.I., 1999. Geotectonic significance of detrital chromian spinel: a review. Geosciences Journal 3, 23-29. doi: 10.1007/BF02910231.

Lee, Y.I., 2009 Geochemistry of shales of the Upper Cretaceous Hayang Group, SE Korea: Implications for Provenance and source weathering at an active continental margin. Sedimentary Geology 215, 1-12. doi: 10.1016/j.sedgeo.2008.12.004.

Lenaz, D., Kamenetsky, S.V., Crawford, J.A., Princivalle, F., 2000. Melt inclusions in detrital spinel from the SE Alps (Italy-Slovenia): a new approach to provenance studies of sedimentary basins. Contributions to Mineralogy and Petrology 139, 748-758. doi: 10.1007/s004100000170

Li, S., Yang, X.Y., Sun, W.D. 2015. The Lamandau IOCG deposit, southwestern Kalimantan Island, Indonesia: evidence for its formation from geochronology, mineralogy, and petrogenesis of igneous host rocks. Ore Geology Reviews 68, 43–58. doi: 10.1016/j.oregeorev.2015.01.008.

Liechti, P.R., Roe, F.W., Haile, N.S., 1960. The geology of Sarawak, Brunei and the western part of North Borneo. Geological Survey Department, British Territories in Borneo 3 (1), 360pp.

Liew, T.C., Page, R.W., 1985. U-Pb zircon dating of granitoid plutons from the West Coast Province of Peninsular Malaysia: Journal of the Geological Society 142, 515–526. doi: 10.1144/gsjgs.142.3.0515.

Liu, Z., Wang, H., Hantoro, W.S., Sathiamurthy, E., Colin, C., Zhao, Y., Li J., 2012. Climatic and tectonic controls on chemical weathering in tropical Southeast Asia (Malay Peninsula, Borneo, and Sumatra). Chemical Geology 291, 1–12. doi:10.1016/j.chemgeo.2011.11.015.

Mange, M.A., Maurer, H.F.W., 1992. Heavy Minerals in Colour, Chapman & Hall, London 147pp.

Mange, M.A., Morton, A.C., 2007. Geochemistry of Heavy Minerals. In: Mange, M.A., Wright, D.T. (Eds.), Heavy Minerals in Use. Developments in Sedimentology. 58, pp. 345-391. Elsevier, UK. doi:10.1016/S0070-4571(07)58013-1.

McLennan, S.M., 2001. Relationships between the trace element composition of sedimentary rocks and upper continental crust. Geochemistry, geophysics, geosystems 2, 1021. doi:10.1029/2000GC000109.

McLennan, S.M., Hemming, S., McDaniel, D.K., Hanson, G.N., 1993. Geochemical approaches to sedimentation, provenance and tectonics. Geological Society of America Special Papers 284, 21–40. doi:10.1130/SPE284-p21

Meinhold, G., Kostopoulos, D., Reischmann, T., Frei, D., BouDaher-Fadel, M. K., 2009. Geochemistry, provenance and stratigraphic age of metasedimentary rocks from the eastern Vardar suture zone, northern Greece. Palaeogeography, Palaeoclimatology, Palaeoecology 277(3-4), 199–225. doi: 10.1016/j.palaeo.2009.04.005.

Mongelli, G., Critelli, S., Perri, F., Sonnino, M., Perrone, V., 2006. Sedimentary recycling, provenance and paleoweathering from chemistry and mineralogy of Mesozoic continental red bed mudrocks, Peloritani Mountains, southern Italy. Geochemical Journal 40,197–209. doi: 10.2343/geochemj.40.197.

Morley, C.K., Back, S., 2008. Estimating hinterland exhumation from late orogenic basin volume, NW Borneo. Journal of the Geological Society London 165(1), 353-366. doi: 10.1144/0016-76492007-067.

Morley, C.K., Back, S., van Rensbergen, P., Crevello, P., Lambiase, J.J., 2003. Characteristics of repeated, detached, Miocene–Pliocene tectonic inversion events, in a large delta province on an active margin, Brunei Darussalam, Borneo. Journal of Structural Geology 25, 1147–1169. doi: 10.1016/S0191-8141(02)00130-X.

Morton, A.C., 1991. Geochemical studies of detrital heavy minerals and their application to provenance studies. In: Morton, A.C., Todd, S. P., Haughton, P.D.W. (Eds.), Developments in Sedimentary Provenance. Geological Society of London, Special Publication. 57, pp.31–45.

Morton, A.C., Fanning, C.M., Jones, N.S., 2010. Variscan sourcing of Westphalian (Pennsylvanian) sandstones in the Canonbie Coalfield, UK. Geological Magazine 147(5), 718-727. doi: 10.1017/S0016756810000014.

Morton, A.C., Hallsworth, C.R., 2007 Stability of detrital heavy minerals during burial diagenesis. In: Mange, M.A., Wright, D.T. (Eds.), Heavy Minerals in Use. Developments in Sedimentology Elsevier, UK, 58, pp.215-245.

Moss, S.J., 1998. Embaluh Group turbitites in Kalimantan: evolution of a remnant oceanic basin in Borneo during the Late Cretaceous to Palaeogene. Journal of the Geological Society London 155, 509-524. doi: 10.1144/gsjgs.155.3.0509.

Moss, S.J., Carter, A., Hurford, A., Baker, S., 1998. A Late Oligocene tectono-volcanic event in east Kalimantan and the implications for tectonics and sedimentation in Borneo. Journal of the Geological Society London 155, 177-192. doi: 10.1144/gsjgs.155.1.0177.

Nagarajan, R., Armstrong-Altrin, J.S., Kessler, F.L., Hidalgo-Moral, E.L., Dodge-Wan, D., Taib, N.I. 2015. Provenance and tectonic setting of Miocene siliciclastic sediments, Sibuti

Formation, northwestern Borneo. Arabian Journal of Geosciences 8, 8549–8565. doi:10.1007/s12517-015-1833-4.

Nagarajan, R., Armstrong-Altrin, J.S., Kessler, F.L., Jong, J., 2017. Petrological and geochemical constraints on provenance, paleo-weathering and tectonic setting of clastic sediments from the Neogene Lambir and Sibuti Formations, NW Borneo. In: Rajat Mazumder, (Ed.), Sediment Provenance: influences on compositional change from source to sink. Elsevier Amsterdam, Netherlands. pp.123-153. (Chapter 7). doi:10.1016/B978-0-12-803386-9.00007-1.

Nagarajan, R., Roy, P.D., Jonathan, M.P., Lozano-Santacruz, R., Kessler F.L., Prasanna M.V., 2014. Geochemistry of Neogene sedimentary rocks from Borneo Basin, East Malaysia: Paleo-weathering, provenance and tectonic setting. Chemie der Erde-Geochemistry 74(1), 139-146. doi: 10.1016/j.chemer.2013.04.003.

Nesbitt, H.W., Young G.M., 1982. Early Proterozoic climates and plate motions inferred from major element chemistry of lutites. Nature 299(5885), 715–717. doi:10.1038/299715a0.

Ng, S.W.P., Whitehouse, M. J., Searle, M. P. Robb, L. J. Ghani, A. A. Chung, S.L., Oliver, G.J.H., Sone, M., Gardiner, N.J., Roselee, M.H., 2015. Petrogenesis of Malaysian granitoids in the Southeast Asian tin belt: Part 2. U-Pb zircon geochronology and tectonic model. Geological Society of America Bulletin 127(9-10), 1238-1258. doi: 10.1130/B31214.1.

Ohta, T., 2008. Measuring and adjusting the weathering and hydraulic sorting effects for rigorous provenance analysis of sedimentary rocks: a case study from the Jurassic Ashikita Group, south-west Japan. Sedimentology 55(6), 1687-1701. doi: 10.1111/j.1365-3091.2008.00963.x.

Pacle, N.A.D., Dimalanta, C.B., Ramos, N.T., Payot, B.D., Faustino-Eslava, D.V., Queaño, K.L., Yumul, G.P. Jr., 2016. Petrography and geochemistry of Cenozoic sedimentary sequences of the southern Samar Island, Philippines: Clues to the unroofing history of an ancient subduction zone. Journal of Asian Earth Sciences. doi:10.1016/j.jseaes.2016.07.030.

Pe-Piper, G., Triantafyllidis, S., Piper, D.J.W., 2008. Geochemical identification of clastic sediment provenance from known sources of similar geology: the Cretaceous Scotian Basin, Canada. Journal of Sedimentary Research 78(9), 595–607. doi: 10.2110/jsr.2008.067.

Pober, E., Faupl, P., 1988. The chemistry of detrital chromian spinels and its implications for the geodynamic evalution of the eastern Alps. Geologische Rundschau 77, 641-670.

Potter, P.E., Maynard, J.B., Depetris, P.J., 2005. Mud and Mudstones: Introduction and Overview. Springer Berlin, Heidelberg, New York, 297pp. ISBN 3-540-22157-3.

Proenza, J.A., Zaccarini, F., Escayola, M., Cábana, C., Schalamuk, A., Garuti, G., 2008. Composition and textures of chromite and platinum-group minerals in chromitites of the western ophiolitic belt from Pampean Ranges of Córdoba, Argentina. Ore Geology Review 33, 32-48. doi: 10.1016/j.oregeorev.2006.05.009.

Rahman, M.J.J., Suzuki, S. 2007. Geochemistry of sandstones from the Miocene Surma group, Bengal Basin, Bangladesh: implications for provenance, tectonic setting and weathering. Geochemical Journal 41, 415–428.

Rangin, C., Bellon, H., Benard, P., Letouzey, J., Muller, C., Sanudin, T., 1990. Neogene arc-continent collision in Sabah, Northern Borneo (Malaysia). Tectonophysics 183, 305–319. doi: 10.1016/0040-1951(90)90423-6.

Ratcliffe, K.T., Morton, A., Ritcey, D., Evenchick, C.E., 2007. Whole rock geochemistry and heavy mineral analysis as exploration tools in the Bowser and Sustut Basins, British

Colombia, Canada. Journal of Canadian Petroleum Geology 55, 320-337. doi: 10.2113/gscpgbull.55.4.320.

Roser, B.P., Korsch, R.J., 1986. Determination of tectonic setting of sandstone-mudstone suites using SiO_2 content and K_2O/Na_2O ratio. Journal of Geology 94, 635-650.

Roser, B.P., Korsch, R.J., 1988. Provenance signatures of sandstone–mudstone suites determined using discrimination function analysis of major element data. Chemical Geology 67, 119–139. doi: 10.1016/0009-2541(88)90010-1.

Roy, P.D., Morton-Bermea, O., Hernández-Álvarez, E., Pi, T., Lozano, R., 2010. Rare earth element geochemistry of the Late Quaternary tephra and volcano-clastic sediments from the Pachuca sub-basin, north-eastern Basin of Mexico. Geofisica International 49, 3–15.

Ryan, K.M., Williams, D.M., 2007. Testing the reliability of discrimination diagrams for determining the tectonic depositional environment of ancient sedimentary basins. Chemical Geology 242(1–2), 103–125. doi: 10.1016/j.chemgeo.2007.03.013.

Sahoo, P.K., Souza-Filho, P.W.M., Guimarães, J.T.F., da Silva, M.S., Costa, F.R., Manes, C.L.D.O., Oti, D., Júnior, R.O.S., Dall'Agnol, R., 2015. Use of multi-proxy approaches to determine the origin and depositional processes in modern lacustrine sediments: Carajás Plateau, Southeastern Amazon, Brazil. Applied Geochemistry 52, 130-146. doi: 10.1016/j.apgeochem.2014.11.010.

Searle, M.P., Whitehouse, M.J., Robb, L.J., Ghani, A.A., Hutchison, C.S., Sone, M., Ng, S.W.P., Roselee, M.H., Chung, S.L., Oliver, G.J.H., 2012. Tectonic evolution of the Sibumasu-Indochina terrane collision zone in Thailand and Malaysia: Constraints from new U-Pb zircon chronology of SE Asian tin granitoids. Journal of the Geological Society 169, 489–500. doi: 10.1144/0016-76492011-107.

Sevastjanova, I., Hall, R., Alderton, D., 2012. A detrital heavy mineral viewpoint on sedimentary provenance and tropical weathering in SE Asia. Sedimentary Geology 280, 179–194. doi: 10.1016/j.sedgeo.2012.03.007.

Sláma, J., Kosler, J., Condon, D.J., Crowley, J.L., Gerdes, A., Hanchar, J.M., Horstwood, M.S.A., Morris, G.A., Nasdala, L., Norberg, N., Schaltegger, U., Schoene, B., Tubrett, M.N., Whitehouse, M.J. 2008. Plesovice zircon - A new natural reference material for U-Pb and Hf isotopic microanalysis. Chemical Geology 249(1-2), 1-35. doi: 10.1016/j.chemgeo.2007.11.005.

Stern, G., Wagreich, M., 2013. Provenance of the Upper Cretaceous to Eocene Gosau Group around and beneath the Vienna Basin (Austria and Slovakia). Swiss Journal of Geosciences 106, 505–527. doi: 10.1007/s00015-013-0150-8.

Sun, S-s., McDonough, W.F., 1989. Chemical and isotopic systematics of oceanic basalts : Implications of mantle composition and processes. Geological Society of London Special Publication 42, 313–345. doi:10.1144/GSL.SP.1989.042.01.19.

Tanean, H., Paterson, D.W., Endharto, M., 1996. Source Provenance interpretation of Kutei basin sandstones and the implication for tectonostratigraphic evolution of Kalimantan. Indonesian Petroleum Association, Proceedings of the 25th Annual Convention. Jakarta, 25, 333–345.

Taylor, S.R., McLennan, S.M., 1985. The continental crust: Its composition and evolution. Oxford: Blackwell Scientific Publications. Carlton, 312pp.

Tongkul, F., 1997. Sedimentation and tectonics of Paleogene sediments in central Sarawak. Bulletin of the Geological Society of Malaysia 40, 135-155.

Totten, M.W., Hanan, M.A., Weaver, B.L., 2000. Beyond whole-rock geochemistry of shales: The importance of assessing mineralogic controls for revealing tectonic discriminants of multiple sediment sources for the Ouachita Mountain flysch deposits. Geological Society of America Bulletin 112 (7), 1012–1022.

Van Hattum, M.W.A, Hall, R., Pickard, A.L., Nichols, G.J., 2013. Provenance and geochronology of Cenozoic sandstones of northern Borneo. Journal of Asian Earth Sciences 76, 266–282. doi: 10.1016/j.jseaes.2013.02.033.

Van Hattum, M.W.A., Hall, R., Nichols, G.J., 2003. Provenance of northern Borneo Sediments. In: Indonesian Petroleum Association, Proceedings 29th Annual Convention and Exhibition, Jakarta, IPA03-G-016: pp. 305-319.

Van Hattum, M.W.A., Hall, R., Pickard, A.L., Nichols, G.J., 2006. SE Asian sediments not from Asia: provenance and geochronology of North Borneo sandstones. Geology 34, 589–592.

Verma, S.P, Armstrong-Altrin, J.S., 2016. Geochemical discrimination of siliciclastic sediments from active and passive margin settings. Sedimentary Geology 332, 1-12. doi: 10.1016/j.sedgeo.2015.11.011.

Verma, S.P., Armstrong-Altrin, J.S., 2013. New Multi-Dimensional Diagrams for Tectonic Discrimination of Siliciclastics Sediments and their Application to Precambrian Basins. Chemical Geology 355, 117-133. doi:10.1016/j.chemgeo.2013.07.014.

Verma, S.P., Lozano-Santa Cruz, R., Girón, P., Velasco, F., 1996. Calibración preliminarde Fluorescencia de Rayos X para análisis cuantitativo de elementos trazas enrocas ígneas. Actas INAGEQ 2, 231–242.

Von Eynatten, H., Tolosana-Delgado, R., Karius, V., 2012. Sediment generation in modern glacial settings: grain-size and source-rock control on sediment composition. Sedimentary Geology 280, 80-92. doi:10.1016/j.sedgeo.2012.03.008.

Wan, H.M., Chen, S.H., 1988. Mineralogical and chemical studies of gravel weathering and its relation to lateritic soil formation in the Linkou terrace. Ti-Chih 8, 22-47 (in Chinese).

Weltje, G.J., Von Eynatten, H., 2004. Quantitative provenance analysis of sediments: review and outlook. Sedimentary Geology, 171(1-4), 1-11. doi: 0.1016/j.sedgeo.2004.05.007.

White, L.T., Graham, I., Tanner, D., Hall, R., Armstrong, R.A., Yaxley, G., Barron, L., Spencer, L., van Leeuwen, T.M., 2016. The provenance of Borneo's enigmatic alluvial diamonds: A case study from Cempaka, SE Kalimantan. Gondwana Research 38, 251-272. doi: 10.1016/j.gr.2015.12.007.

Williams, P.R., Johnston, C.R., Almond, R.A., Simamora, W.H., 1988. Late Cretaceous to Early Tertiary structural elements of West Kalimantan: Tectonophysics 178, 279–297.

Witts, D., Hall, R., Nichols, G., Morley, R., 2012. A new depositional and provenance model for the Tanjung Formation, Barito Basin, SE Kalimantan, Indonesia. Journal of Asian Earth Sciences 56, 77–104. doi: 10.1016/j.jseaes.2012.04.022.

Zaid, S.M., 2015. Integrated petrographic, mineralogical, and geochemical study of the Late Cretaceous–Early Tertiary Dakhla Shales, Quseir–Nile Valley Province, central Egypt: implications for source area weathering, provenance, and tectonic setting. Arabian Journal of Geosciences 8(11), 9237-9259. doi:10.1007/s12517-015-1875-7.

Zhang, L., Qin, X., Liu, J., Sun, C., Mu, Y., Gao, J., Guo, W., An, S., Lu, C., 2016. Geochemistry of sediments from the Huaibei Plain (east China): Implications for provenance,

weathering, and invasion of the Yellow River into the Huaihe River. Journal of Asian Earth Sciences 121, 72–83. doi: 10.1016/j.jseaes.2016.02.008.

Figure Captions

Figure 1 Map showing geology and location of the study area: (A) geology of the northwestern Borneo (after Liechti et al., 1960), (B) location of the Tukau Formation, and (C) stratigraphy of the present study with sample locations.

Figure 2 Geochemical classification of clastic sedimentary rocks of the Tukau Formation (after Herron, 1988).

Figure 3 Upper Continental Crust (UCC; McLennan, 2001) normalised major oxides and trace elements in different sedimentary rocks of the Tukau Formation.

Figure 4 Chondrite normalized REE (Sun and McDonough, 1989) patterns of sedimentary rocks from the Tukau Formation.

Figure 5 Bulk mineralogy (in wt %) of sedimentary rocks from the Tukau Formation analysed in QEMSCAN

Figure 6 Distribution of heavy minerals in one arkose (S02) and two different wacke (S07 and S14) from the Tukau Formation analysed in SEM, Optical microscopy and QEMSCAN.

Figure 7a-i Morphological features of heavy minerals present in sedimentary rocks from the Tukau Formation (Zr= Zircon; Rut = Rutile; Tour = Tourmaline; Mon = Monazite; Cr = Chromian spinel; Ilm = Ilmenite)

Figure 8 (a) Conventional U-Pb Concordia plots (total zircons and younger age zircons: data point error ellipses are 2σ) of the U-Pb isotoic analyses results obtained from the Laser ablation, and (b) relative frequency plots of youngest zircon ages obtained for the Tukau Formation.

Figure 9 Sedimentary rocks of the Tukau Formation in Al_2O_3 - (CaO* +Na_2O) - K_2O (A-CN-K; after Nesbitt and Young, 1982) ternary diagram.

Figure 10 Al_2O_3-Zr-TiO_2 plot showing sorting trend for the sedimentary rocks from the Tukau Formation (after Garcia et al., 1994).

Figure 11 Major oxide based provenance discrimination plot of Roser and Korsch (1988) for sedimentary rocks from the Tukau Formation.

Figure 12 Hf vs. La/Th bi-plot of sedimentary rocks from the Tukau Formation after Floyd and Leveridge, 1987).

Figure 13 Composition of detrital tourmalines in (a) Ca-Fe_{total}-Mg ternary diagram and (b) Al-Fe_{total}-Mg ternary diagram of Henry and Guidotti (1985).

Figure 14 Chemical composition of chromian spinels in (a) Al_2O_3 versus Cr_2O_3 diagram after Bonavia et al. (1993) (b) Trivalent major cation plot (Fe^{3+}–Al^{3+}–Cr^{3+}) after Cookenboo et al. (1997), (c) variation of Mg# against Cr# of detrital chromian spinels. Fields of spinels are reconstructed after Pober and Faupl, (1988) and (d) Al_2O_3 vs TiO_2 (Wt%) in chromian spinels

from sediments of the Tukau Formation. The discrimination fields of chromian spinel from Kamenetsky et al. (2001).

Figure 15 SiO_2 vs K_2O/Na_2O plot shows the tectonic setting discrimination fields for Tukau Formation sedimentary rocks (after Roser and Korsch, 1986).

Figure 16 (a) Discrimination diagrams based on major element (oxides) and (b) major and trace elements (after Verma and Armstrong-Altrin, 2016) for the Tukau Formation sedimentary rocks.

Table Captions

Table 1 Summary of major and trace element concentrations of the sedimentary rocks, Tukau Formation.

Table 2 Mineralogy of whole rock (WR) and clay fraction (<2μm) of sedimentary rocks from the Tukau Formation obtained with XRD.

Table 3 Composition of heavy minerals (Tourmaline, Chromian Spinel and Garnet) from sedimentary rocks of the Tukau Formation.

Supplementary Files

1. Detailed methodology for QEMSCAN and heavy mineral analyses
2. Table 1 QEMSCAN bulk mineralogy (in %) of the sedimentary rocks of Tukau Formation, East Malaysia.

3. Table 2 Whole rock geochemistry results for sedimentary rocks of the Tukau Formation.
4. Table 3 Geochemical results of tourmaline, chromian spinels and garnet grains separated from sedimentary rocks of the Tukau Formation.

Figure 1

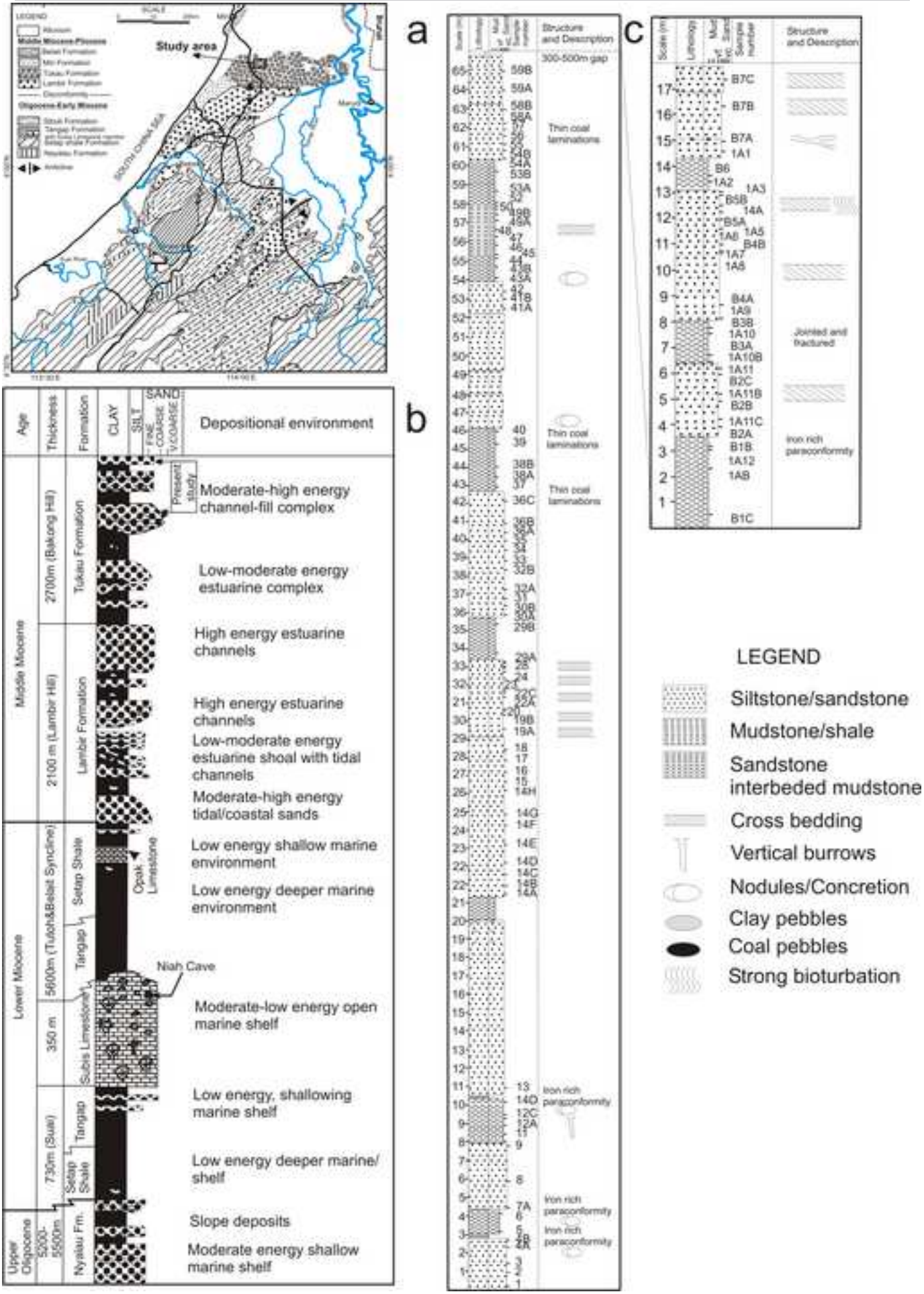

Figure 2

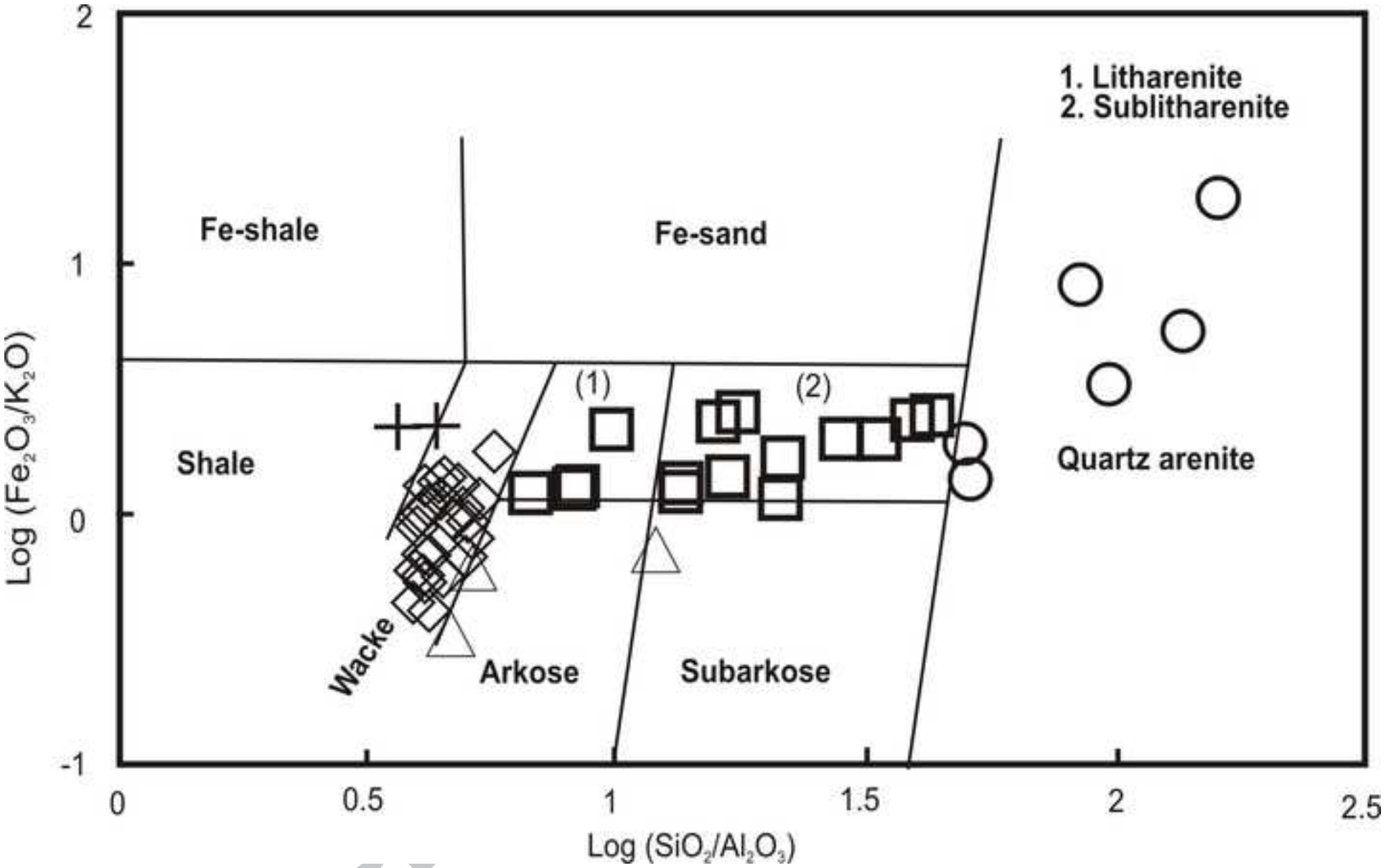

Figure 3

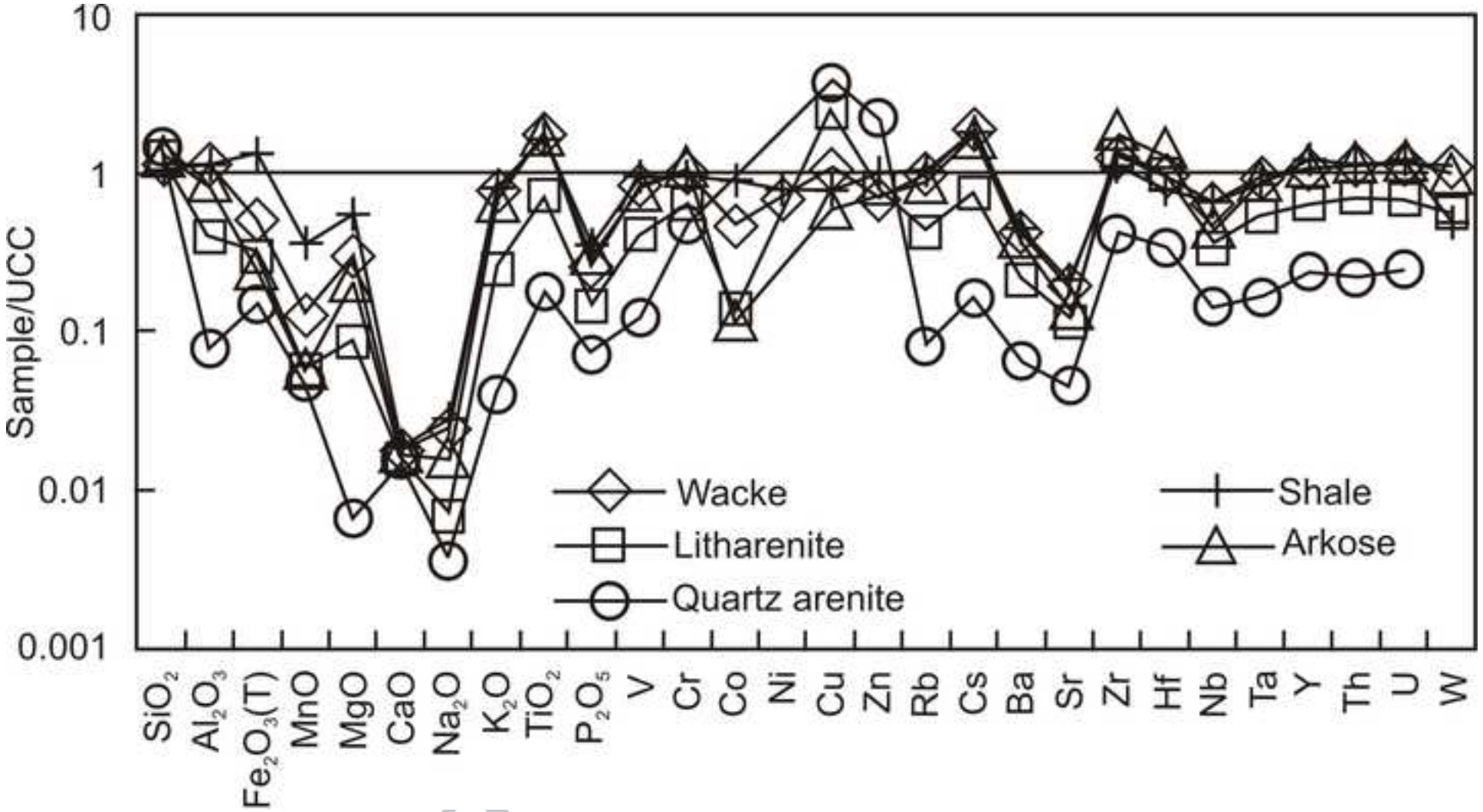

Figure 4

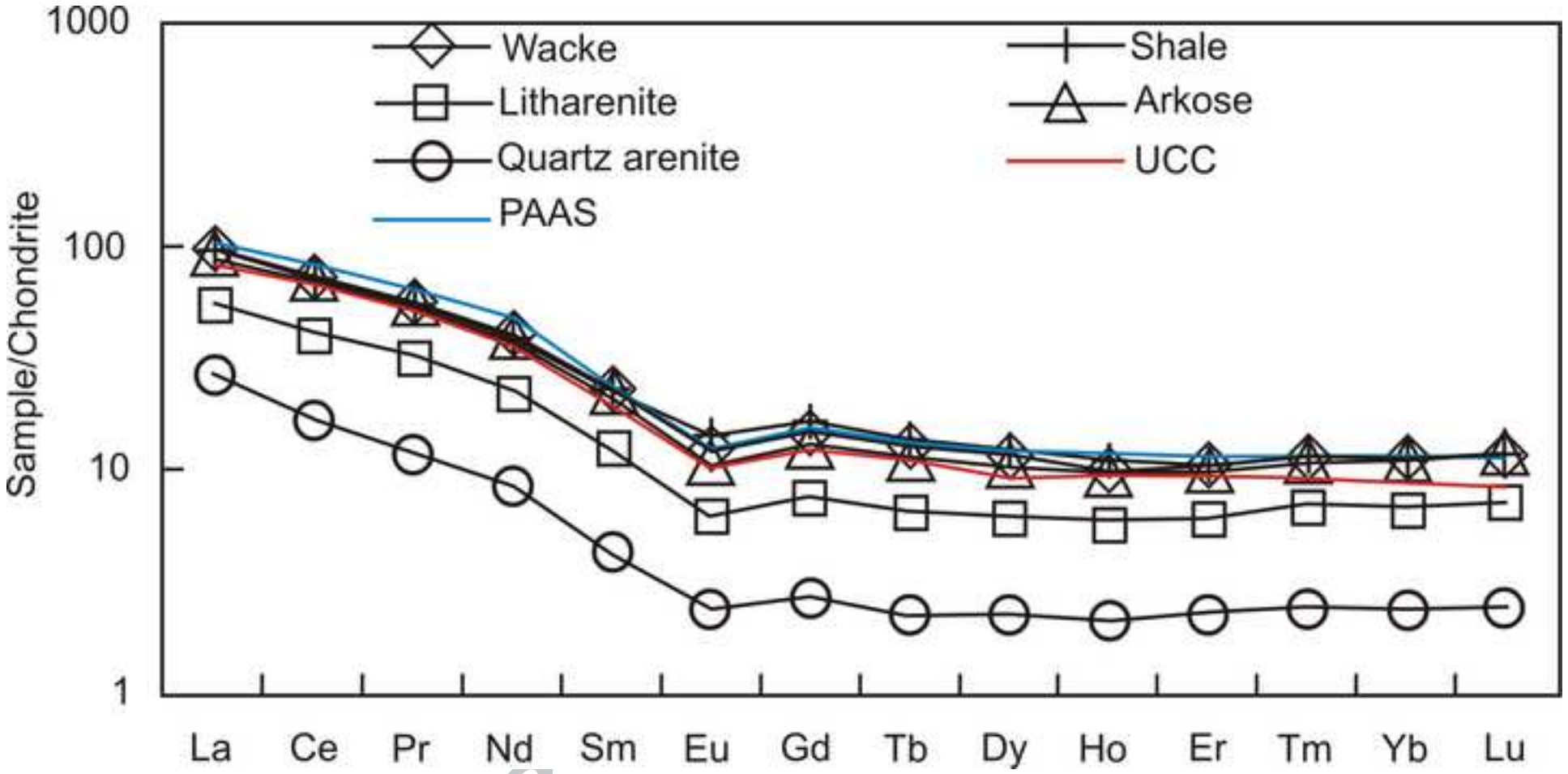

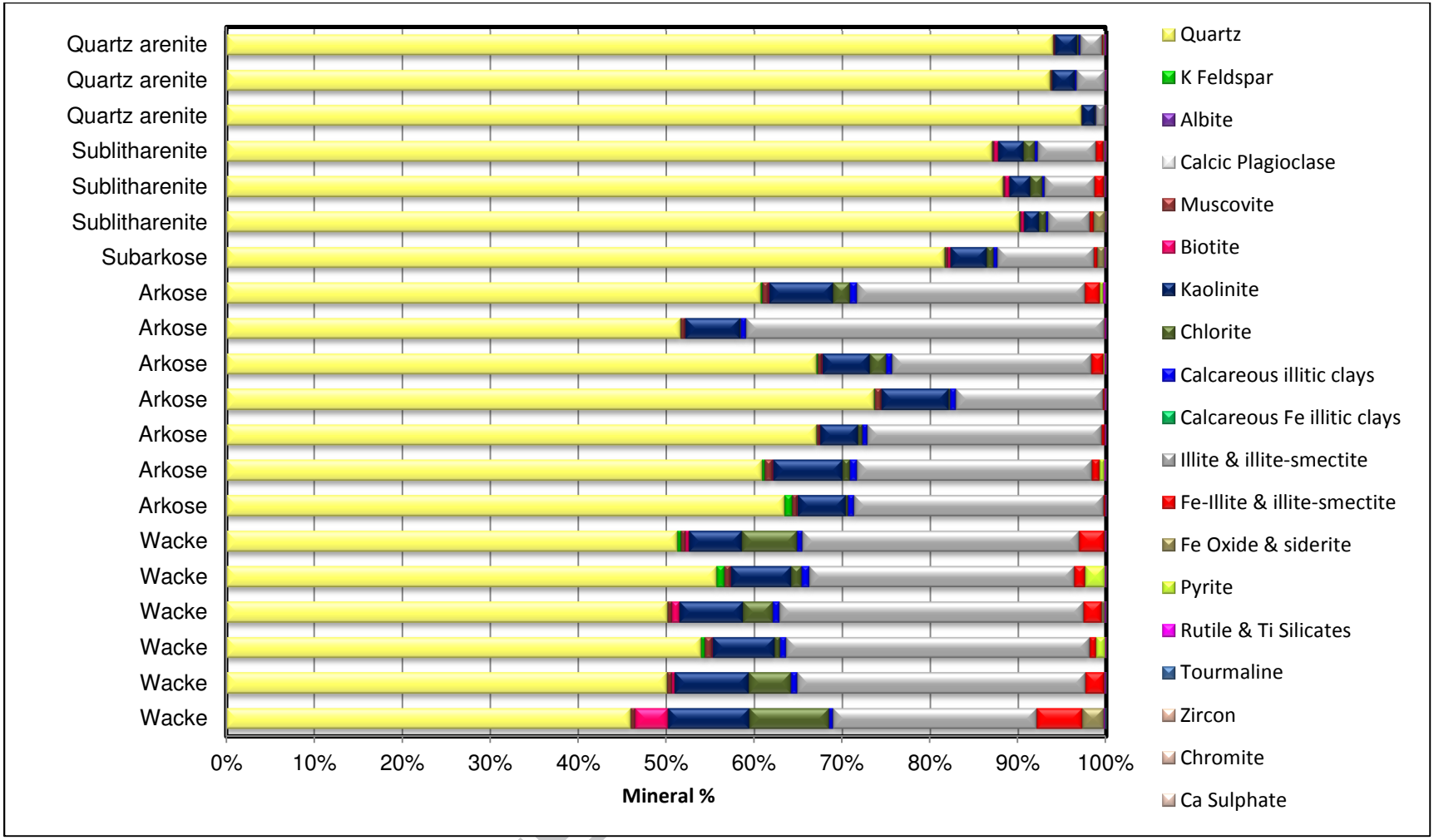

Figure 5

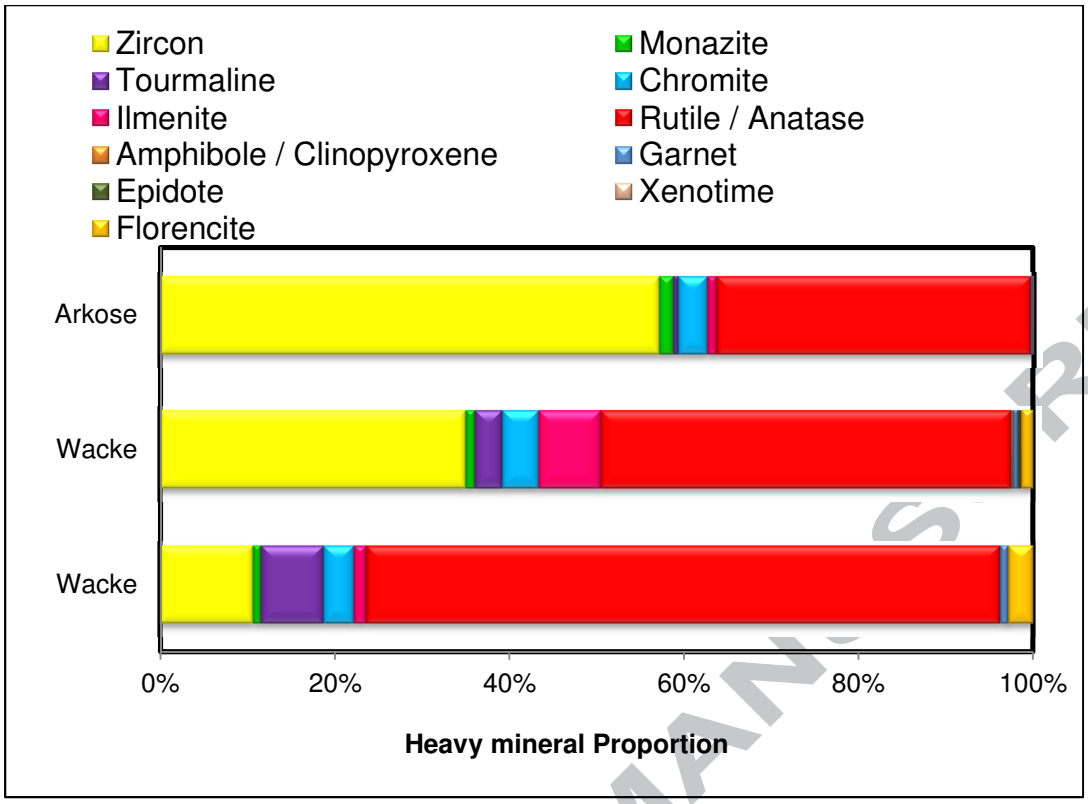

Figure 6

Figure 7

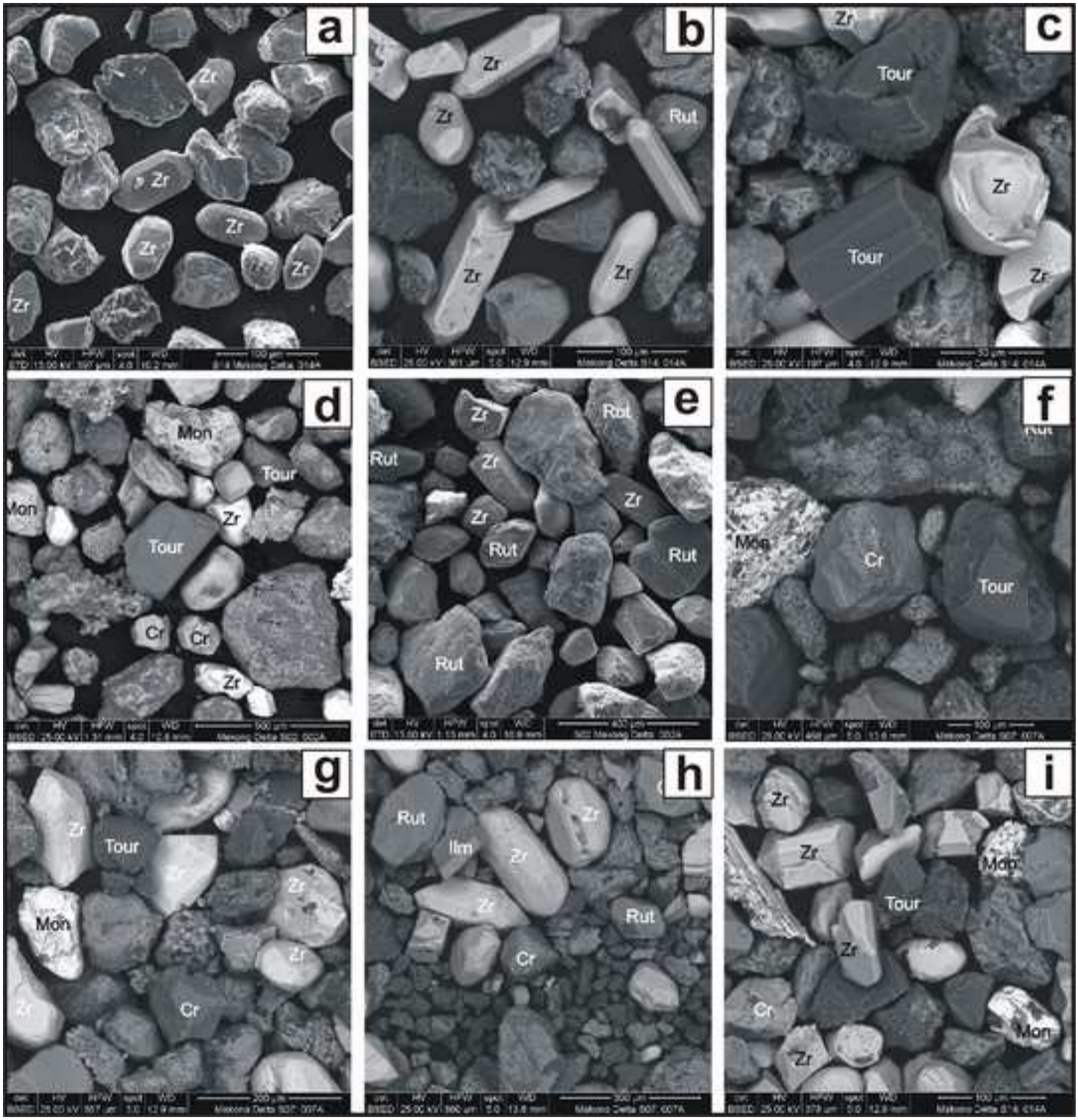

Figure 8

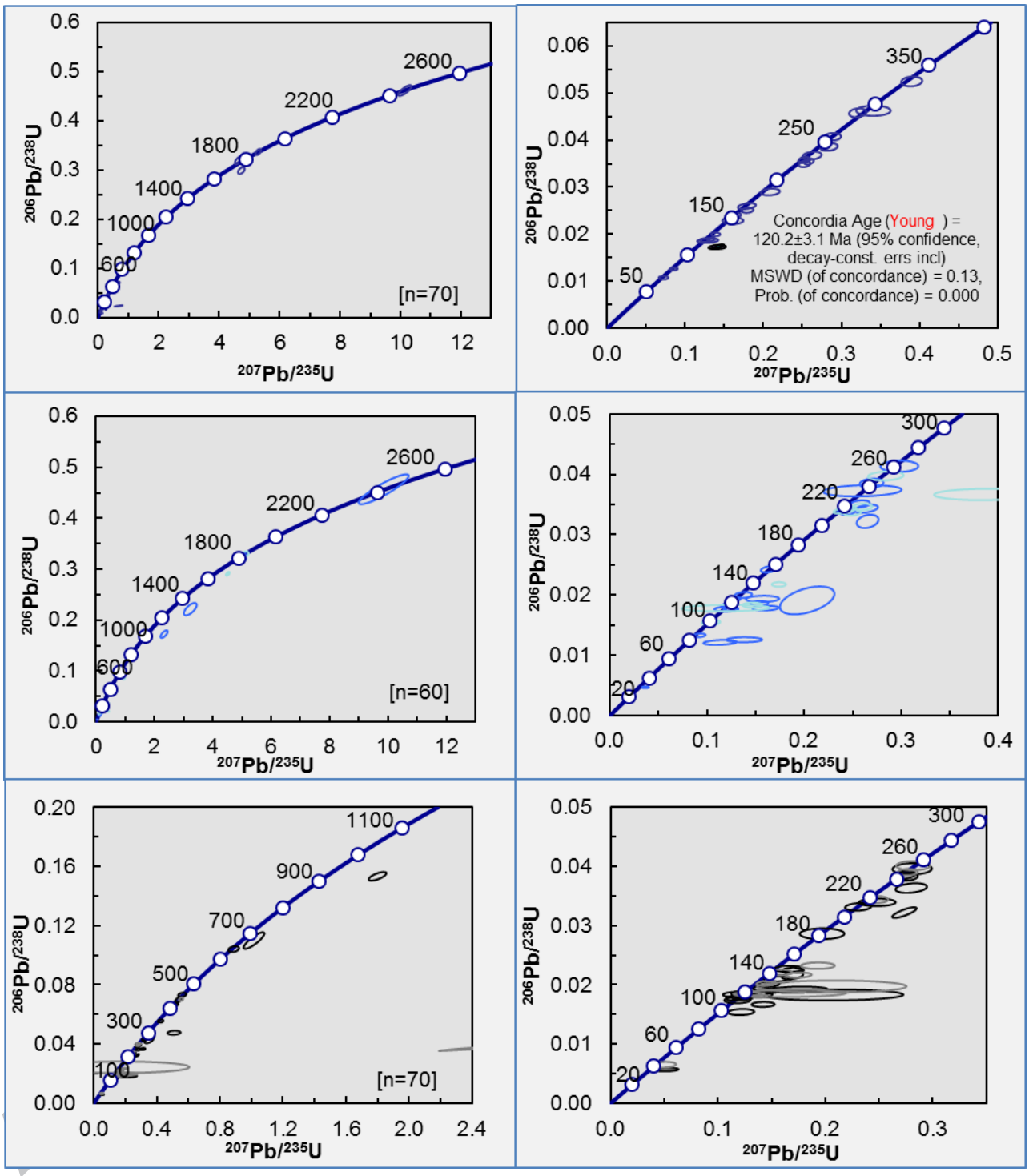

Figure 8a

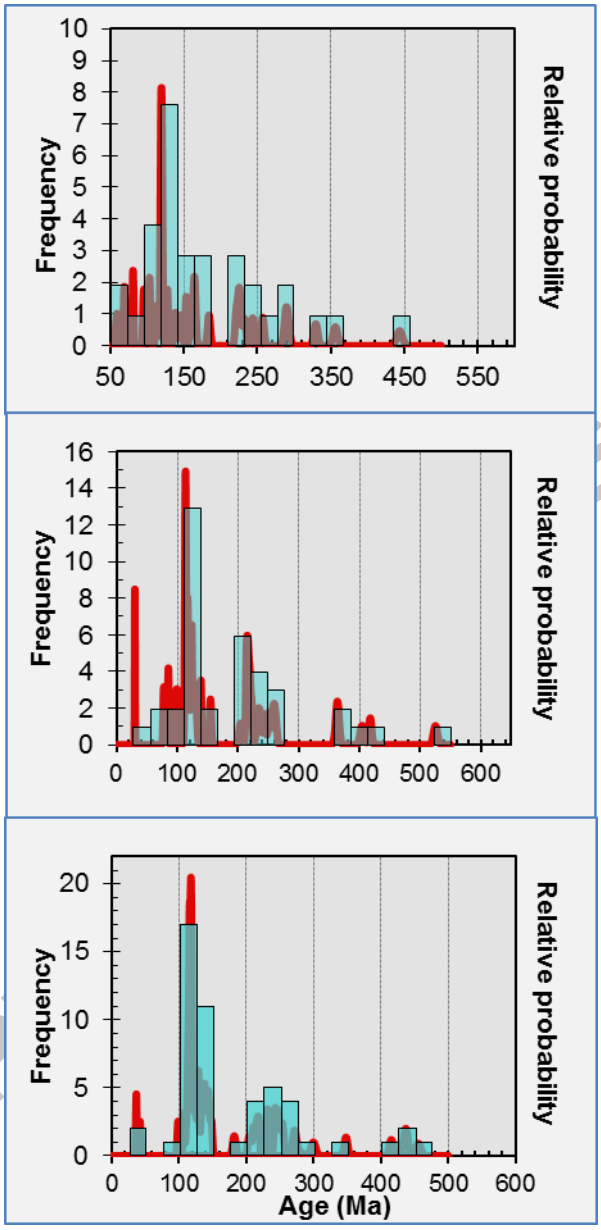

Figure 8b

Figure 9

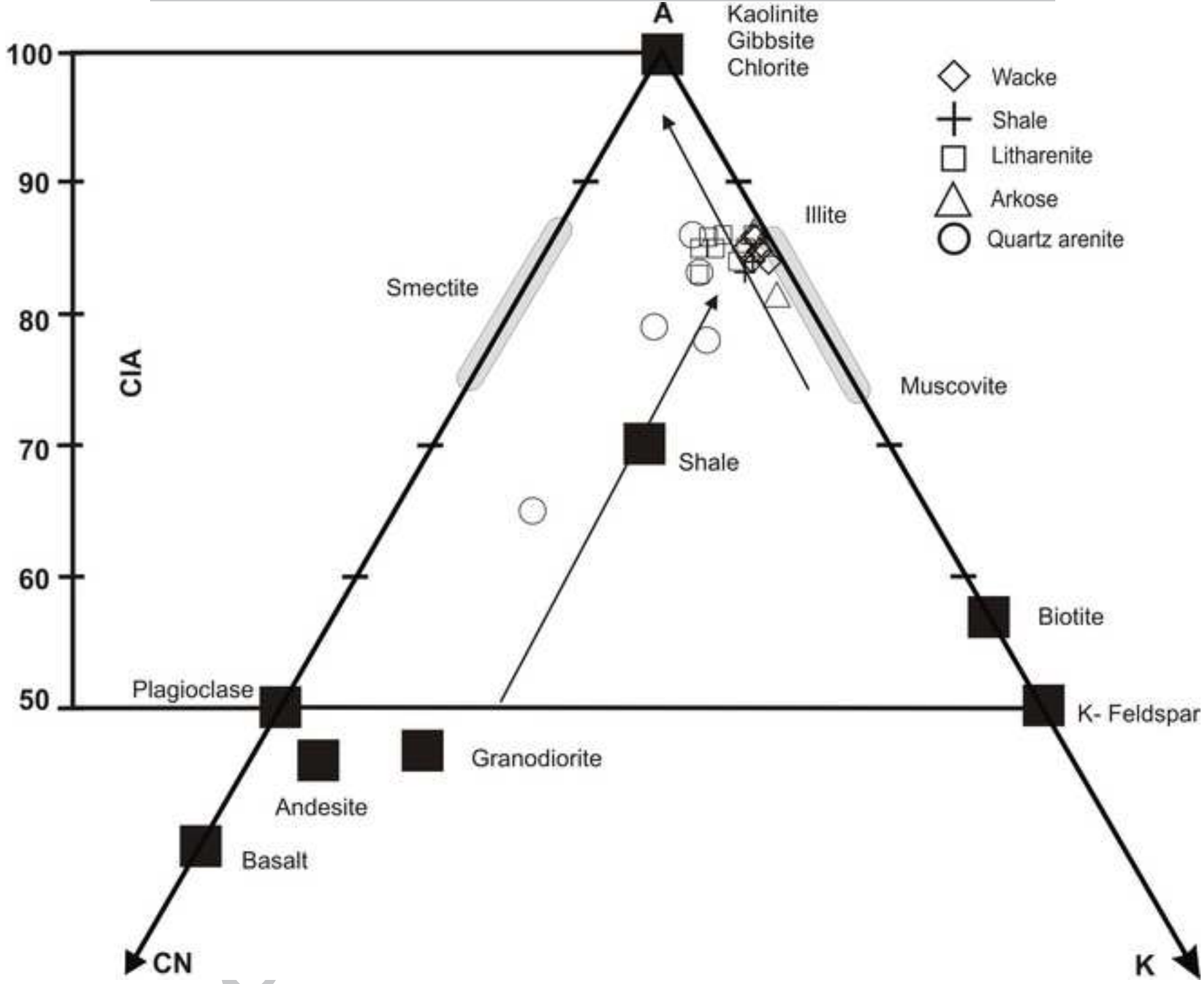

Figure 10

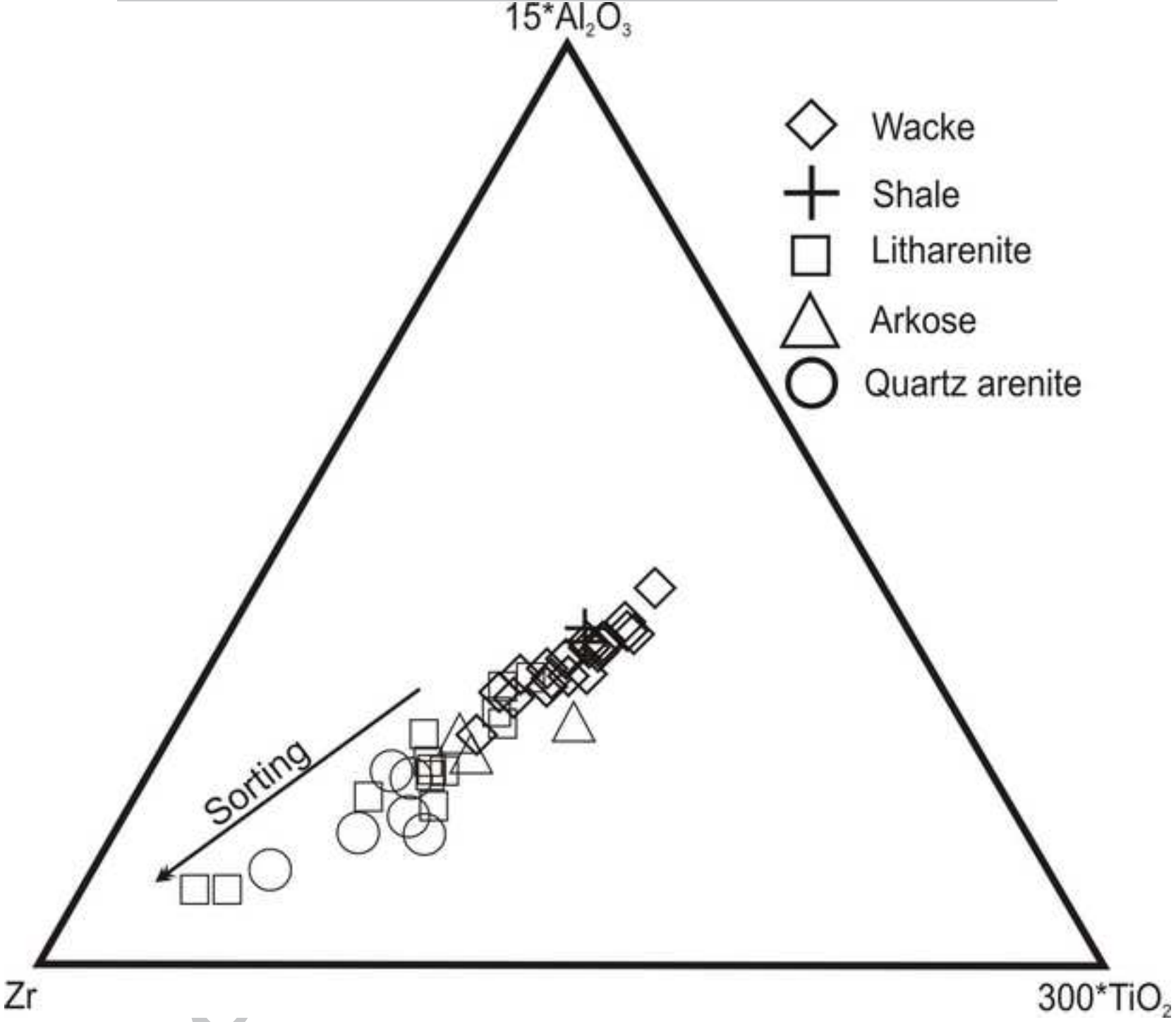

Figure 11

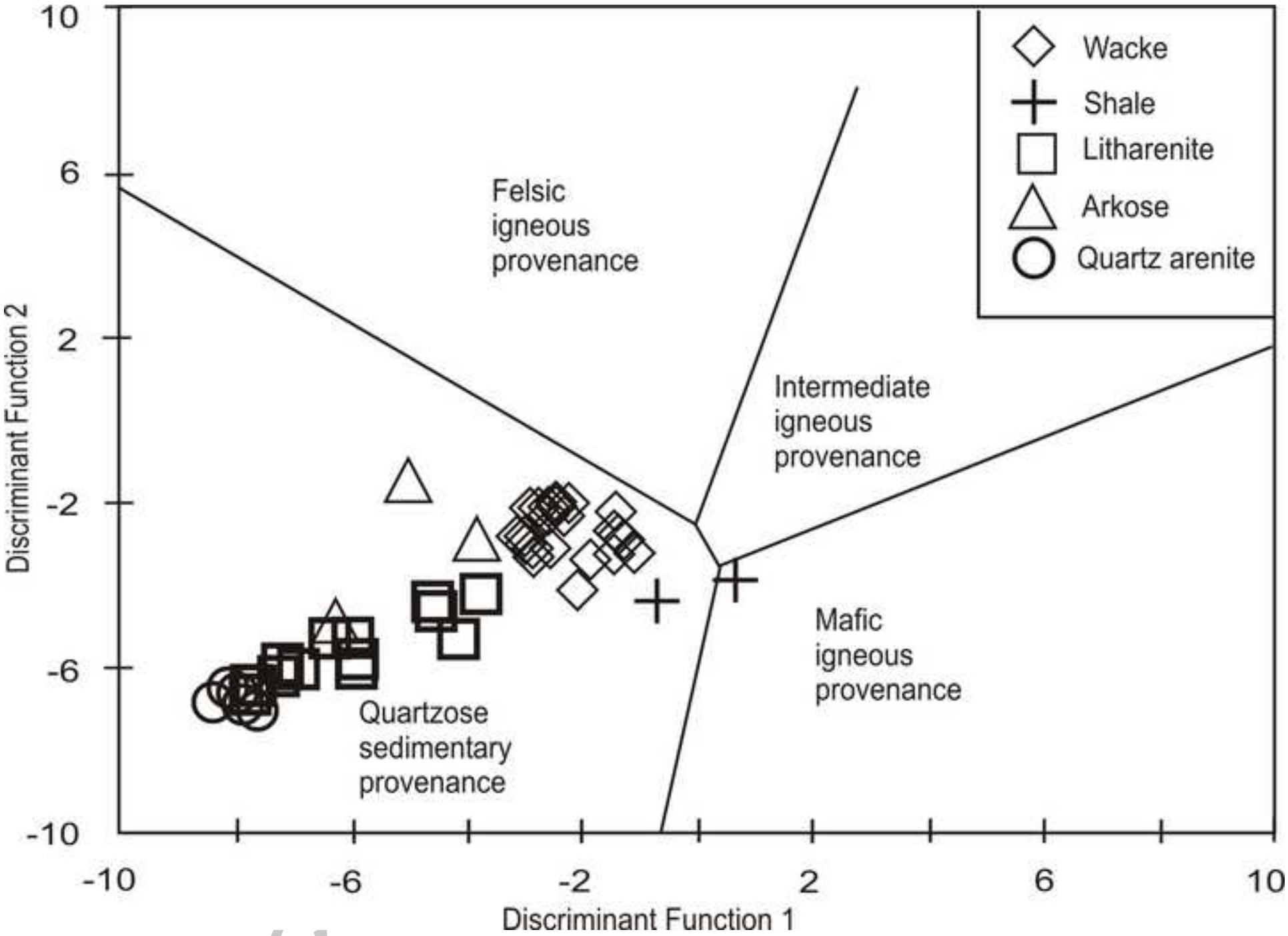

Figure 12

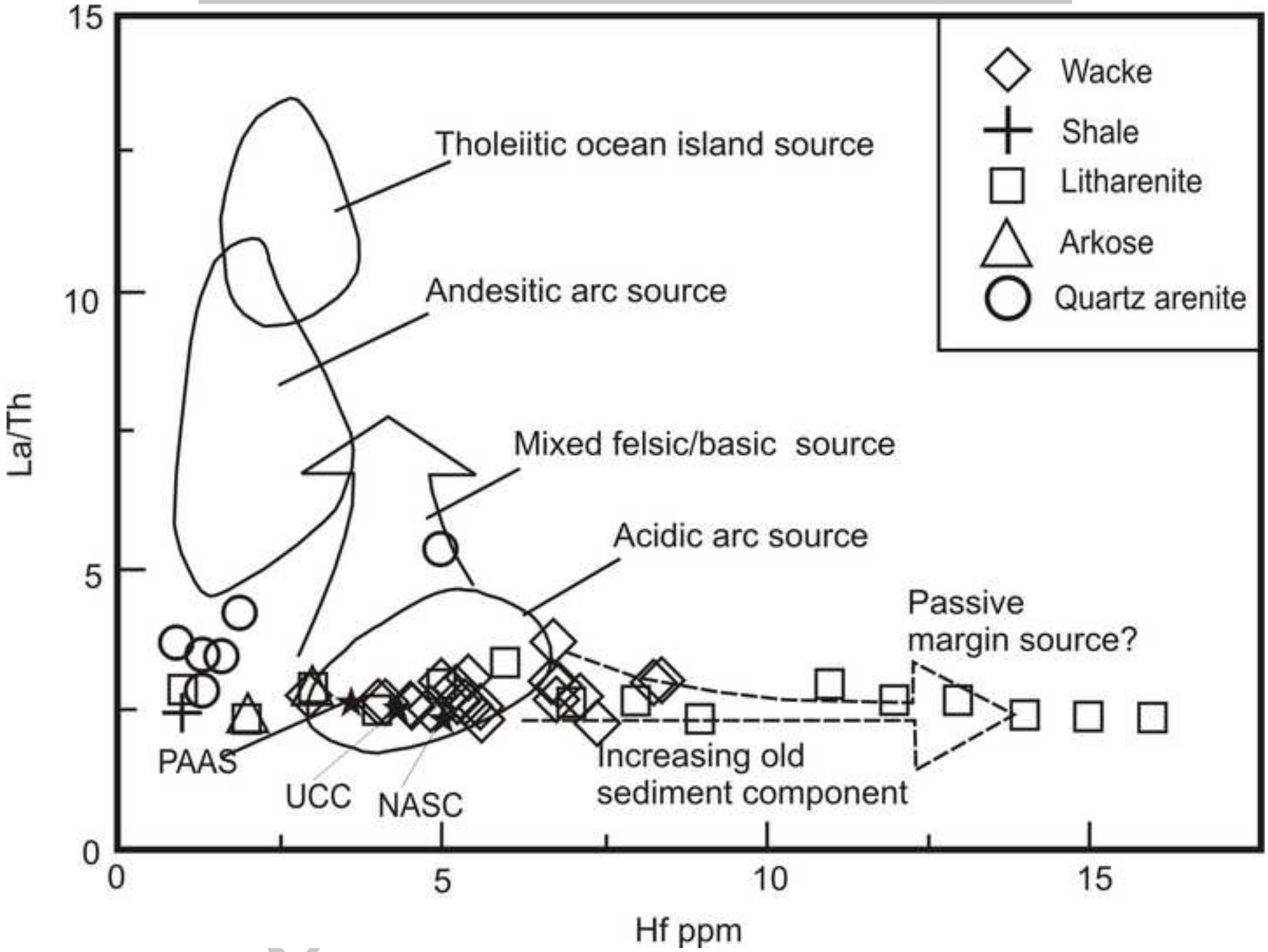

Figure 13

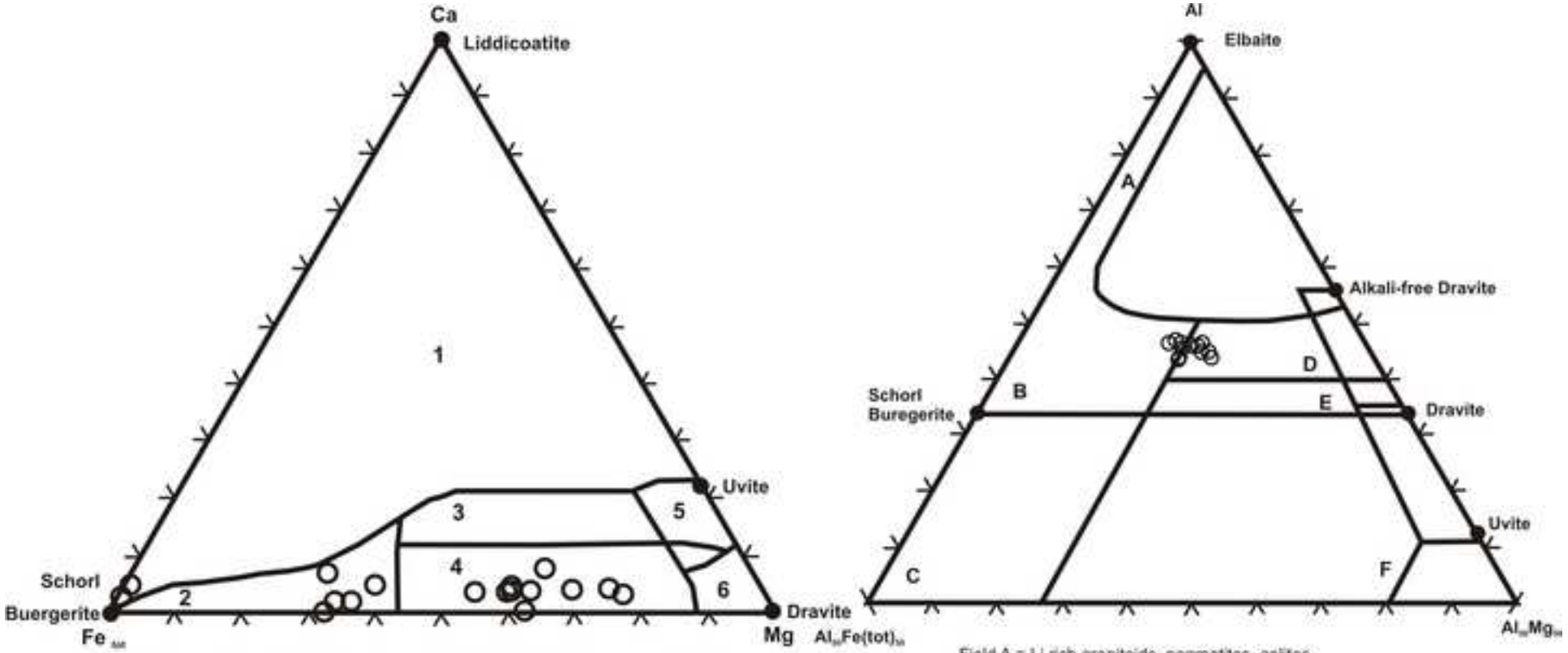

Compositional fields (Hendry and Guidotti, 1995; Preston et al. 2002)
1 = Li rich granitoids, pegamatites and aplites
2 = Li poor granitoids, pegamatites and aplites
3 = Ca rich metapelites, metapsammites and calc-silicates
4 = Ca poor metapelites, metapsammites and calc-silicates
5 = metacarbonates; 6 = metapyroxenites

Field A = Li rich granitoids, pegmatites, aplites
Field B = Li poor granitoids, pegmatites, aplites
Field C = hydrothermally altered granitic rocks
Field D = metapelites, metapsammites (aluminous)
Field E = metapelites and metapasamites (Al-Poor)
Field F = Fe^{3+} -rich quartz-tourmaline rocks, calc-silicates, metapelites

Figure 14

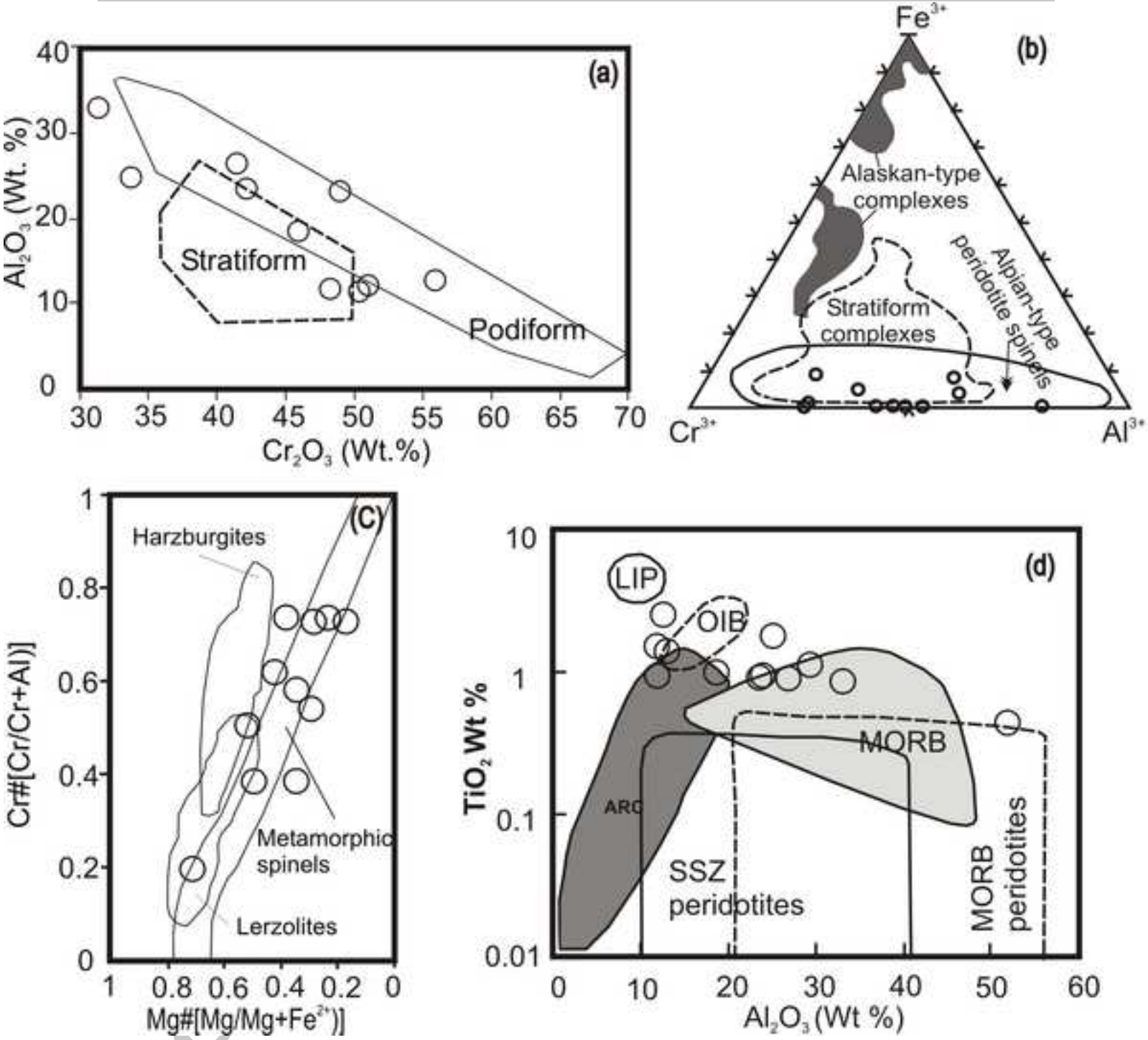

Figure 15

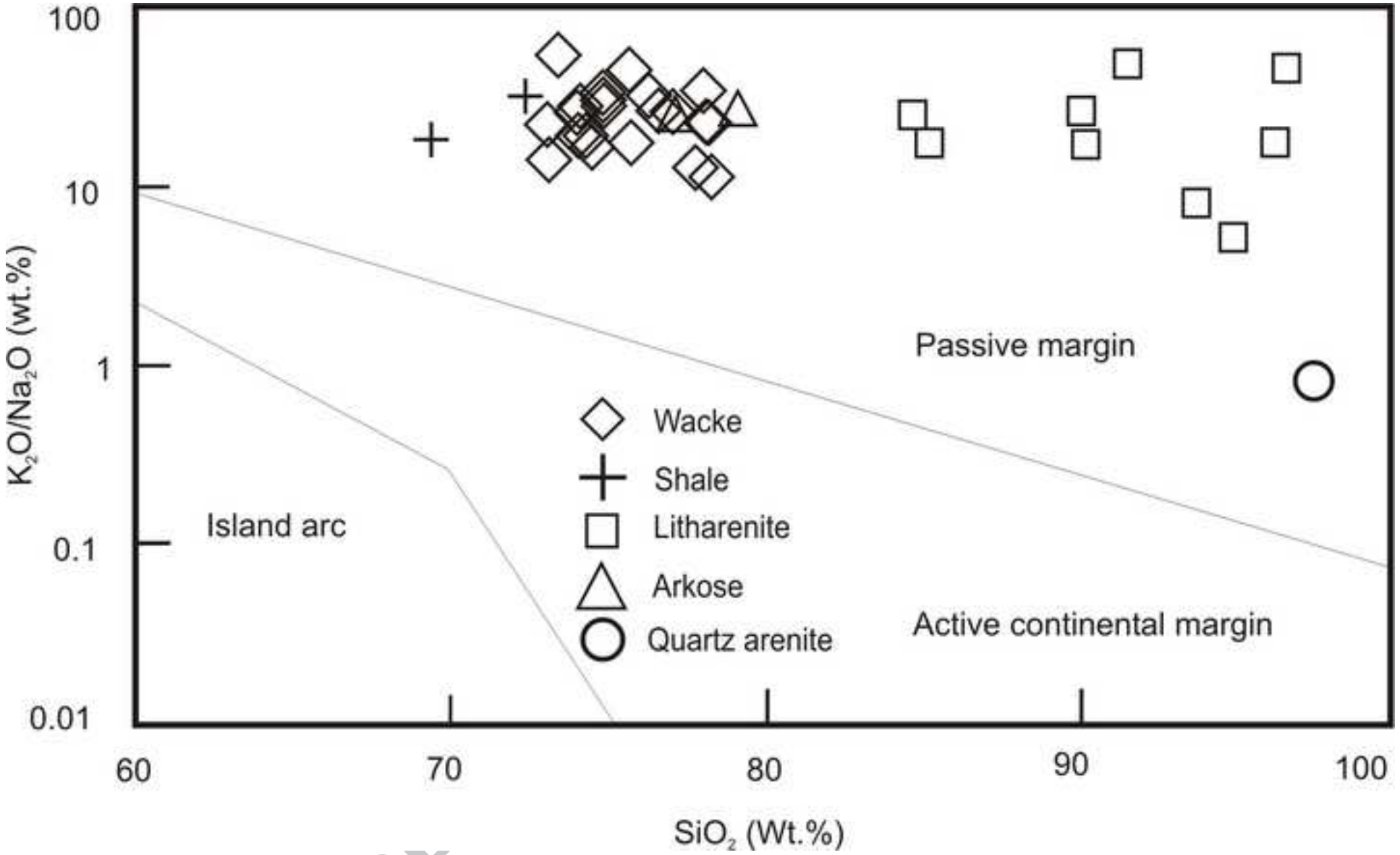

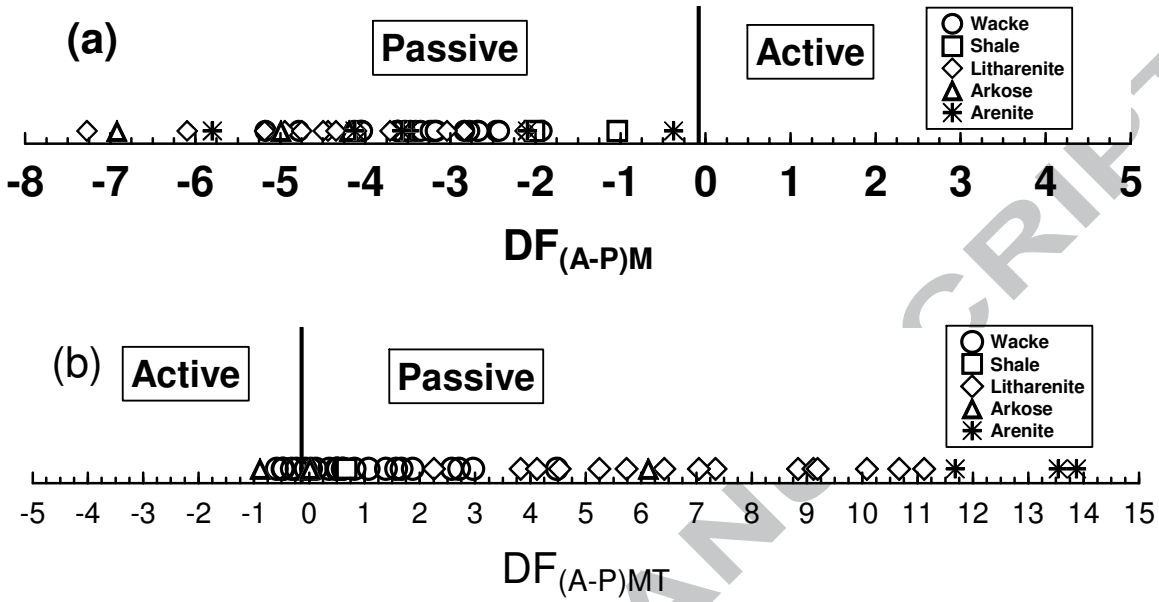

Figure 16

Table 1

Oxide	Wacke (n=24)		Shale (n=2)		Litharenites (n=15)		Arkoses (n=3)		Arenite (n=6)	
(%)	Range	Avg	Range	Avg.	Range	Avg	Range	Avg	Range	Avg
SiO_2	66.25-75.16	70.90	62.57 -66.43	64.50	80.20 - 96.19	89.67	74.13 -89.06	79.31	96.89 -98.45	97.75
$SiO_{2(adj)}$	73.01-78.61	75.60	69.26 -72.33	70.80	82.72- 96.59	90.93	77.14 -89.71	81.98	97.28 -98.67	97.75
TiO_2	0.73 - 0.95	0.85	0.75 - 0.77	0.76	0.11- 0.68	0.36	0.50 -1.19	0.84	0.06 -0.16	0.09
Al_2O_3	13.20 - 18.06	16.47	15.38 -17.19	16.29	2.22- 12.02	6.02	7.54 -15.97	12.69	0.60 -1.96	1.23
Fe_2O_3t	1.11 - 3.59	2.20	5.52 - 5.80	5.66	0.62- 2.60	1.37	0.80 -1.37	1.05	0.32 -1.57	0.70
MnO	0.004 - 0.021	0.009	0.023 -0.029	0.026	0.001 -0.009	0.004	0.001 -0.007	0.004	0.002 -0.006	0.004
MgO	0.41 - 1.12	0.63	1.12 -1.12	1.12	0.05 -0.41	0.19	0.16 -0.59	0.43	0.00 -0.04	0.01
CaO	0.06 - 0.10	0.07	0.07 -0.07	0.07	0.06 -0.09	0.07	0.07 -0.07	0.07	0.05 -0.07	0.06
Na_2O	0.00 - 0.19	0.09	0.07 -0.13	0.10	0.00 -0.08	0.03	0.00 -0.10	0.06	0.00 -0.09	0.01
K_2O	1.91 - 2.83	2.50	2.42 -2.61	2.51	0.25 -1.65	0.84	1.12 -3.01	2.13	0.07 -0.23	0.14
P_2O_5	0.03 - 0.06	0.04	0.05 -0.06	0.06	0.01 -0.04	0.02	0.03 -0.06	0.04	0.01 -0.02	0.01
Element										
(ppm)	99.35 - 101.10	100.19	99.91 -100.23	100.07	98.96 -100.96	100.41	99.81 -100.37	100.14	99.98 -100.93	100.49
V	35.00 - 119.00	93.96	96.00 -108.00	102.00	19.00 -83.00	44.60	67.00 -90.00	82.33	5.00 -22.00	13.20
Cr	40.00 - 230.00	84.58	80.00 -80.00	80.00	20.00 -80.00	53.85	80.00 -90.00	86.67	40.00 -40.00	40.00
Co	1.00 - 28.00	8.17	15.00 -16.00	15.50	1.00 -7.00	2.43	1.00 -3.00	2.00	-	-
Ni	20.00 - 40.00	31.67	30.00 -40.00	35.00	-	-	-	-	-	-
Cu	10.00 - 50.00	27.50	20.00 -20.00	20.00	10.00 -260.00	63.33	10.00 -20.00	15.00	20.00 -170.00	95.00
Zn	30.00 - 110.00	50.00	50.00 -100.00	75.00	40.00 -100.00	57.50	-	-	160.00 -160.00	160.00
Ga	6.00 - 21.00	16.92	16.00 -18.00	17.00	3.00 -15.00	8.27	13.00 -17.00	15.33	2.00 -4.00	2.60
Ge	1.00 - 2.00	1.36	1.00 - 1.00	1.00	1.00 -2.00	1.20	1.00 -1.00	1.00	1.00 -1.00	1.00
As	5.00 - 11.00	7.40	6.00 - 7.00	6.50	5.00 -16.00	8.70	5.00 -6.00	5.50	19.00 -19.00	19.00
Rb	32.00 - 142.00	114.71	114.00 -122.00	118.00	13.00 -84.00	48.60	77.00 -111.00	98.33	4.00 -19.00	9.33
Sr	23.00- 89.00	63.46	74.00 -75.00	74.50	14.00 -70.00	41.00	42.00 -54.00	48.67	9.00 -31.00	16.17
Y	9.00 - 44.00	25.04	24.00 -32.00	28.00	6.00 -25.00	14.33	19.00 -27.00	24.00	3.00 -8.00	5.33
Zr	126.00 -369.00	246.83	205.00 -205.00	205.00	60.00 -749.00	250.00	244.00 -439.00	342.00	37.00 -209.00	79.00
Nb	4.00 -10.00	7.75	5.00 -11.00	8.00	2.00 -8.00	4.20	4.00 -6.00	5.33	1.00 -3.00	1.75
Sn	2.00 - 6.00	2.52	1.00 - 2.00	1.50	1.00 -3.00	1.89	1.00 -2.00	1.67	1.00 -1.00	1.00
Cs	2.60 -11.40	8.98	8.40 - 9.00	8.70	0.90 -6.70	3.59	6.00 -9.30	7.70	0.50 -1.20	0.78
Ba	77.00 -293.00	240.00	243.00 -262.00	252.50	40.00 -204.00	118.27	180.00 -230.00	213.00	24.00 -62.00	35.83
Hf	2.90 - 8.40	5.70	4.50 - 5.00	4.75	1.60 -16.90	5.75	5.60 -9.70	7.57	0.90 -5.00	2.00
Ta	0.40 - 1.20	0.96	0.80 - 0.90	0.85	0.20 -0.90	0.55	0.70 -1.00	0.90	0.10 -0.30	0.17
W	1.00 -11.00	2.25	1.00 - 1.00	1.00	1.00 -2.00	1.14	2.00 -2.00	2.00	-	-
Tl	0.30 - 0.50	0.43	0.30 - 0.40	0.35	0.10 -0.30	0.20	0.20 -0.40	0.33	-	-
Pb	9.00 -60.00	20.21	13.00 -14.00	13.50	6.00 -21.00	11.57	12.00 -29.00	21.33	5.00 -11.00	7.50
Th	4.50 -16.50	12.60	11.80 -13.80	12.80	3.50 -13.10	7.63	11.60 -13.10	12.43	1.30 -4.60	2.33
U	1.10 - 4.00	3.21	3.40 - 3.60	3.50	0.80 -3.40	2.09	2.90 -3.80	3.37	0.50 -1.20	0.70
La	12.70 -42.50	35.39	31.20 -35.20	33.20	9.60 -31.60	20.33	28.50 -39.20	34.43	4.90 -25.00	9.85
Ce	24.60 -90.00	69.99	61.90 -70.70	66.30	17.50 -63.00	39.26	55.30 -80.20	68.43	8.60 -37.30	16.48
Pr	2.79 -10.80	7.85	6.96 - 8.14	7.55	1.97 -6.97	4.41	6.07 -8.98	7.64	0.96 -3.11	1.65
Nd	10.70 -42.70	28.87	25.70 -30.70	28.20	7.10 -25.60	16.03	21.80 -33.80	28.13	3.60 -11.40	6.00
Sm	2.00 -10.50	5.45	4.90 - 6.40	5.65	1.20 -4.50	2.91	4.10 -6.30	5.20	0.60 -2.00	1.02
Eu	0.39 - 2.51	1.14	1.08 - 1.40	1.24	0.20 -0.90	0.55	0.73 -1.21	0.96	0.12 -0.40	0.21
Gd	1.70 -10.60	4.55	4.30 - 5.90	5.10	1.00 -3.50	2.32	2.70 -5.00	3.97	0.50 -1.40	0.83
Tb	0.30 - 1.60	0.73	0.70 - 0.90	0.80	0.20 -0.60	0.39	0.50 -0.80	0.67	0.10 -0.30	0.14
Dy	1.50 - 9.00	4.42	4.10 - 5.50	4.80	1.00 -3.80	2.35	3.20 -4.60	4.07	0.60 -1.40	0.87
Ho	0.30 - 1.60	0.88	0.80 - 1.10	0.95	0.20 -0.80	0.49	0.70 -0.90	0.83	0.10 -0.30	0.18
Er	1.00 - 4.40	2.70	2.50 - 3.10	2.80	0.60 -2.60	1.53	2.00 -2.90	2.57	0.40 -0.90	0.57
Tm	0.15 - 0.62	0.41	0.39 - 0.45	0.42	0.10 -0.42	0.24	0.32 -0.48	0.41	0.05 -0.14	0.09
Yb	1.00 - 4.00	2.80	2.70 - 2.90	2.80	0.60 -3.00	1.68	2.30 -3.30	2.87	0.40 -1.00	0.60
Lu	0.16 - 0.59	0.45	0.40 - 0.48	0.44	0.09 -0.49	0.27	0.39 -0.53	0.47	0.06 -0.18	0.10

Table 2

Mineral/ Sample No	Fraction	S1 Arkose	S04 Arkose	S08 Arkose	S12 Arkose	S13 Arkose	S06 Wacke	S09 Wacke
Quartz	WR	86.69	82.95	97.33	93.07	79.19	80.69	86.69
(wt %)	-2 µm	18.4	28.3	6.1	44.3	26	55.7	23.6
Kaolinite (wt%)	WR	1.89	1.49	0.82	1.47	1.69	1.799	1.36
	-2 µm	49.7	15.2	46	15.8	24.4	15.301	27.5
	Crystallinity	Poor	Mod	Poor	Poor	Poor	Mod	Mod
Illite (wt%)	WR	11.42	15.54	1.85	5.46	19.12	16.65	11.75
	-2 µm	28.7	46.92	47.9	38.8	49.1	26.2	45.9
	Crystallinity	Poor	Mod	Mod	Mod	Mod	Mod	Mod
Smectite	WR	-	-	-	-	-	-	-
(wt %)	-2 µm	Tr	9.6	Tr	0.2	0.5	-	3
Pyrite	WR	-	-	-	-	-	0.86	0.2
(wt %)	-2 µm	-	-	-	-	-	2.8	-
Jarosite	WR	-	-	-	-	-	-	-
(wt %)	-2 µm	3.2	-	Tr	0.9	-	-	-
Total	WR	100	100	100	100	100	100	100
(wt%)	-2 µm	100	100	100	100	100	100	100

WR= whole rock; Tr=trace; - = not detected; Mod = moderate

Table 3

Tourmalines (n=17)			Chromian Spinels (n=12)			Garnets (n=2)		
Parameters	Range	Avg	Parameters	Range	Avg.	Parameters	Range	Avg
SiO_2	32.2-37.0	34.7	SiO_2	0-6.0	0.8	SiO_2	30.9-34.6	32.78
TiO_2	0-4.4	1.5	TiO_2	0.4-2.5	1.2	TiO_2	0-1.1	0.54
Al_2O_3	33.1-46.9	42.2	Al_2O_3	11.8-51.8	23.4	Al_2O_3	21.7-24.9	23.28
Cr_2O_3	-	-	Cr_2O_3	19.3-55.9	41.3	Cr_2O_3	0	0.00
FeO	6.1-18.5	11.6	FeO	11.8-35.4	25.5	FeO	5.3-29.2	17.24
Fe_2O_3	-	-	Fe_2O_3	-	-	Fe_2O_3	0.2-2.5	1.34
MnO	0	0	MnO	0	0	MnO	0-34.2	17.12
MgO	0-12.5	6.6	MgO	0-16.6	7.7	MgO	0-9.8	4.90
CaO	0-1.7	0.7	CaO	0	0	CaO	1.3-4.5	2.94
Na_2O	0-5.1	2.7	Na_2O	0	0	Na_2O	0	0
Atomic ratio	stoichiometric calculation based on 24.5O		Atomic ratio	stoichiometric calculation based on 4O		Atomic ratio	stoichiometric calculation based on 12O inc. Fe_2/Fe_3	
Si	4.7-5.3	5.0	Si	0-0.2	0.1	Si	2.6 - 2.7	2.65
Ti	0-0.5	0.17	Ti	0.01-0.06	0.03	Ti	0-0.1	0.03
Al	5.9-7.8	7.2	Al	0.5-1.7	0.9	Al	2.1-2.3	2.2
Fe	0.7-2.5	1.4	Cr	0.4-1.5	1.1	Cr	0	0
Fe^{3+}	-	-	Fe^{3+}	0.0-0.2	0.04	Fe^{3+}	0.01-0.2	0.1
Fe^{2+}	-	-	Fe^{2+}	0.3-0.9	0.6	Fe^{2+}	0.4-1.9	1.1
Mg	0-2.6	1.4	Mg	0-0.7	0.35	Mg	0-1.1	0.6
Mn	0	0	Mn	0	0	Mn	0-2.4	1.2
Ca	0-0.3	0.1	∑cat.	3.0	3.0	Ca	0.1-0.4	0.3
Na	0-1.5	0.8	∑O.	4.0-4.2	4.0	Total	8.2-8.2	8.2
Total	15.2-16.6	16.1	Cr#	0.2-0.7	0.6	XMn	0-0.8	0.4
Si	4.7-5.3	5.0	Mg#	0.0-0.7	0.4	Almandine	0-53.7	26.8
Al	0.7-1.3	1.0	Fe^{3+}#	0.0-0.1	0.0	Andradite	0.6-9.1	4.8
Fe/(Fe+Mg)	0.2-1.0	0.5	Al^{3+}#	0.2-0.8	0.4	Grossular	0-3.6	1.8
Na/(Na+Ca)	0-1.0	0.6	$Fe^{2+}/(Fe^{2+}+Mg)$	0.3-1.0	0.7	Pyrope	42.2	21.1
Mg/(Fe+Mg)	0-0.8	0.5	Cr#=Cr/(Cr+Al); Mg#=Mg/(Mg+Fe^{2+});			Spessartine	0-90.9	45.5
Al/(Al+Fe+Mg)	0.6-0.8	0.7	$Fe^{3+}=Fe^{3+}/(Fe^{3+}+Cr+Al)$			Alm+Spess	53.7-90.9	72.3

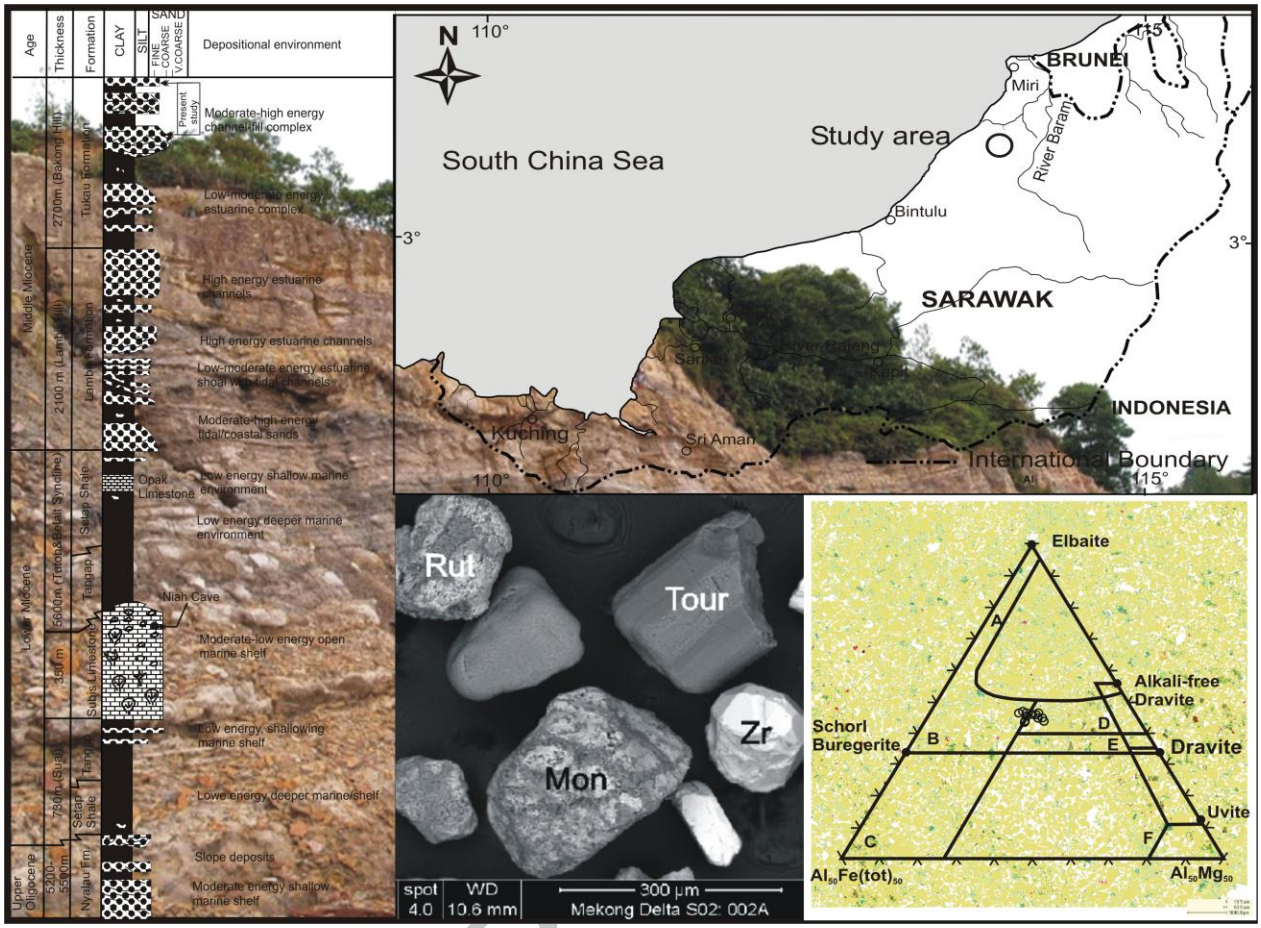
Age
Thickness
Formation
CLAY
SILT
SAND
FINE
COARSE
V.COARSE
Depositional environment
Present study
Moderate-high energy channel-fill complex
Low-moderate energy estuarine complex
High energy estuarine channels
High energy estuarine channels
Low-moderate energy estuarine shoal with tidal channels
Moderate-high energy tidal/coastal sands
Low energy shallow marine environment
Low energy deeper marine environment
Niah Cave
Moderate-low energy open marine shelf
Low energy, shallowing marine shelf
Lowe energy deeper marine shelf
Slope deposits
Moderate energy shallow marine shelf
Middle Miocene
Lower Miocene
Upper Oligocene
2700m (Bakong Hill)
2100 m (Lambir Hill)
5600m (Tatau-Balai Syndline)
350 m
780m (Sujau)
5200-6500m
Tukau Formation
Lambir Formation
Setap Shale
Tangap
Subis Limestone
Setap Shale
Nyalau Fm
Opak Limestone
N
110°
115°
3°
South China Sea
Study area
BRUNEI
Miri
River Baram
Bintulu
SARAWAK
Sarikei
River Rajang
Kapit
INDONESIA
Kuching
Sri Aman
International Boundary
Rut
Tour
Zr
Mon
spot
4.0
WD
10.6 mm
300 µm
Mekong Delta S02: 002A
Elbaite
Alkali-free Dravite
Schorl Buregerite
Dravite
Uvite
A
B
C
D
E
F
$Al_{50}Fe(tot)_{50}$
$Al_{50}Mg_{50}$

Highlights

- Integrated approach to infer weathering, provenance and tectonic setting of the Tukau Formation.
- High maturity and moderate to intensively weathered sedimentary rocks.
- The Schwaner Mountains and Tin Belt of the Malaysia Peninsular were principal provenances.
- Minor contribution from the mafic and ultramafic rocks.
- Deposition in a passive margin with passive collisional and rift settings.